

Gaussian Process-Based Nonlinear Moving Horizon Estimation

Tobias M. Wolff, Victor G. Lopez, *Member, IEEE*, and Matthias A. Müller, *Senior Member, IEEE*

Abstract—In this paper, we propose a novel Gaussian process-based moving horizon estimation (MHE) framework for unknown nonlinear systems. In the proposed scheme, we take advantage of the properties of Gaussian processes. On the one hand, we approximate the system dynamics by the posterior means of the learned Gaussian processes (GPs). On the other hand, we exploit the posterior variances of the Gaussian processes to design the weighting matrices in the MHE cost function and account for the uncertainty in the learned system dynamics. The data collection and the tuning of the hyperparameters are done offline. We prove robust stability of the GP-based MHE scheme using a Lyapunov-based proof technique. Furthermore, as additional contribution, we analyze under which conditions incremental input/output-to-state stability (a nonlinear detectability notion) is preserved when approximating the system dynamics using, e.g., machine learning techniques. Finally, we illustrate the performance of the GP-based MHE scheme in a simulation case study and show how the chosen weighting matrices can lead to an improved performance compared to standard cost functions.

Index Terms—Gaussian Process, Moving Horizon Estimation, Machine learning, State estimation, Nonlinear detectability, Nonlinear systems

I. INTRODUCTION

MOVING horizon estimation (MHE) [1] is an optimization-based state estimation technique. Loosely speaking, at each time instant, an optimization problem is solved to determine an optimally estimated state sequence, based on the available input/output measurements and a mathematical model of the physical system. The cost function of the optimization problem considers the magnitudes of the estimated process and measurement noise (often called stage costs) as well as the deviation between the initial element of the estimated state sequence and a prior estimate (often called prior weighting). The constraints of the optimization problem guarantee that the system dynamics are satisfied (based on the available mathematical model) and, potentially, that the estimated states and disturbances lie in some predefined sets. Finally, the state estimate at the current time instant is set to the last element of the optimal estimated state sequence. In recent years, strong robust stability guarantees have been obtained for general nonlinear systems [1]–[3].

This project has received funding from the European Research Council (ERC) under the European Union's Horizon 2020 research and innovation programme (grant agreement No 948679).

Tobias M. Wolff, Victor G. Lopez, and Matthias M. Müller are with the Leibniz University Hannover, Institute of Automatic Control, 30167 Hannover, Germany (email: {wolff,lopez,mueller}@irt.uni-hannover.de)

Hence, MHE is crucially based on a mathematical model of the system. Typically, expert knowledge, first principles, or heuristics are used to derive such a model. These approaches can be time-consuming and expensive and will not always result in reliable models. An alternative is to *learn* the mathematical model of the system by using some machine learning technique.

Only a few works have studied the combination of MHE and machine learning techniques. In [4], the authors propose to approximate the solution of the MHE optimization problem by a function that is parameterized using a one-hidden-layer feedforward neural network. This approach reduces the computational burden of the MHE scheme. Furthermore, the authors provide stability guarantees by relying on some technical assumptions. However, the MHE scheme and hence also the stability guarantees heavily rely on model knowledge.

Another approach to combine learning techniques and MHE has been suggested in [5]. The authors propose a so-called primal-dual estimation learning method. Loosely speaking, two functions are learned offline, (i) one function that generates state estimates online and (ii) another function that examines the optimality of the estimates. However, the work considers only linear systems, although MHE has been proven to be particularly powerful for nonlinear systems.

An alternative machine learning technique is Gaussian process (GP) regression. A Gaussian process is defined as a collection of random variables, any finite number of which follows a joint Gaussian distribution [6, Def. 2.1]. The key advantage of Gaussian processes (GPs) is that they provide a measure of how uncertain a predicted function output is (using the posterior variance). GPs have already been frequently used in the area of learning-based control, compare, e.g., [7]–[9].

In the context of state estimation, GPs have recently been used for a joint dynamics and state estimation method [10], where the state estimation is performed by a high-gain observer and the dynamics estimation by GPs. Additionally, interval observers using GPs for partially unknown dynamics (with stability guarantees) have been developed in [11]. Other GP-based estimators were proposed in [12], [13], in particular GP-based extended/unscented Kalman filters (EKF/UKF), where the state transition function and the output map are approximated by GPs. Furthermore, GP-based assumed density filters were suggested in [14] [15, Ch. 4], which do not make use of linearizations (as the GP-based EKF) or finite-sample approximations (as the GP-based UKF).

Jointly using MHE and GPs to perform state estimation has already been suggested in some first application-oriented

works in robotics. For instance, in [16], [17], the authors suggest a state estimation framework, where GPs are used to directly estimate the states and not to approximate the system dynamics. The major drawback of these works is that no theoretical stability analysis is done and that the determination of suitable hyperparameters is not addressed. In [18], the authors suggest to approximate parts of the system dynamics by GPs and to build an MHE based on this hybrid model. However, once again, no stability analysis of the presented scheme is done.

In this work, we propose a novel GP-based MHE framework, which uses GPs to approximate the state transition function and the output map. We exploit the uncertainty quantification provided by GPs to design the weighting matrices in the cost function of the MHE scheme. Furthermore, different from [16]–[18], we prove robust stability of the MHE scheme under mild assumptions. Finally, we show the performance of the GP-based MHE scheme in an illustrative example. Additionally, we compare the performance to different standard model-based MHE schemes (with perfect model knowledge) and to another GP-based scheme, where we also approximate the system dynamics by the posterior means of the learned GPs, but we do not account for the uncertainty in the cost function. We argue that our scheme is a competitive alternative to the mentioned works in the literature, due to its simple setup, the possibility to consider inherent system constraints, and the available stability guarantees. As a last contribution, we show that detectability can be preserved during the learning process as long as some technical assumptions are satisfied.

Note that a preliminary version of parts of this work is available in the conference paper [19]. Compared to [19], we here consider the *propagated* uncertainty in the weighting matrices of the stage costs of MHE optimization problem as well as a prior weighting that depends on the uncertainty related to the prior estimate. Moreover, we improve the stability analysis to obtain less conservative error bounds and analyze in much more detail the behavior of the GP-based MHE scheme in numerical examples. Finally, we analyze how detectability can be preserved when approximating the system dynamics by machine learning techniques.

This paper is organized as follows. In Section II, we explain the setting of this work. In the following Sections III and IV, we introduce the GP-based MHE scheme and present the stability analysis, respectively. The detectability analysis is given in Section V. Finally, we close this paper by an illustrative example and a conclusion in Sections VI and VII, respectively.

II. PRELIMINARIES

The set of integers greater than or equal to $a \in \mathbb{R}$ is denoted by $\mathbb{I}_{\geq a}$. Furthermore, the set of non-negative real numbers is written as $\mathbb{R}_{\geq 0}$. We denote the identity matrix of dimension n by I_n and a diagonal matrix of dimension n with q_1, \dots, q_n on the diagonal entries by $\text{diag}(q_1, \dots, q_n)$. A positive definite matrix P is denoted by $P \succ 0$. For a vector $x = [x_1 \ \dots \ x_n]^\top \in \mathbb{R}^n$ and a positive definite matrix P , the weighted vector norm is denoted by $\|x\|_P = \sqrt{x^\top P x}$. If

$P = I$, we just write $\|x\|$, which denote the Euclidean norm of the vector x . The standard maximum (minimum) eigenvalue of a positive definite matrix P is denoted by $\lambda_{\max}(P)$ ($\lambda_{\min}(P)$) and the maximum generalized eigenvalue of positive definite matrices $P_1 = P_1^\top$ and $P_2 = P_2^\top$ is denoted by $\lambda_{\max}(P_1, P_2)$, i.e., the largest scalar λ satisfying $\det(P_1 - \lambda P_2) = 0$. For two symmetric matrices A, B , $A \preceq B$ means that $B - A$ is positive semidefinite. The (Pontryagin) set difference is denoted by \ominus , i.e., for two sets \mathcal{A}, \mathcal{B} , $\mathcal{A} \ominus \mathcal{B} := \{a \in \mathbb{R}^n | a + b \in \mathcal{A}, \forall b \in \mathcal{B}\}$. For some scalar $a \in \mathbb{R}$, we write $\lfloor a \rfloor$ to denote the largest integer less than or equal to a . For two square positive definite matrices of the same dimensions A, B , we define

$$\min(A, B) := \begin{cases} A, & \text{if } A - B \preceq 0 \\ B, & \text{otherwise.} \end{cases}$$

GPs are typically used to approximate some nonlinear function $\bar{f} : \mathbb{R}^{n_d} \rightarrow \mathbb{R}$. They are fully defined by a mean function $m : \mathbb{R}^{n_d} \rightarrow \mathbb{R}$ and a covariance function $k : \mathbb{R}^{n_d} \times \mathbb{R}^{n_d} \rightarrow \mathbb{R}$ (also referred to as kernel). For some $d, d' \in \mathbb{R}^{n_d}$, we write

$$\bar{f}(d) \sim \mathcal{GP}(m(d), k(d, d'))$$

to denote that the function \bar{f} is a random function described by a GP. For simplicity, in the following we consider a zero prior mean function and the squared exponential kernel, as typically done in the context of GPs, compare [6]. Nevertheless, our results hold for any kernel that leads to a continuously differentiable posterior mean. Next, we collect regression input data, which we denote by $D^{dt} = [d_1^{dt} \ \dots \ d_N^{dt}]$ and regression output data $Y^{dt} = [y_1^{dt} \ \dots \ y_N^{dt}]^\top$, where the regression output y^{dt} is given by $y^{dt} = \bar{f}(d^{dt}) + \varepsilon^{dt}$ and $\varepsilon^{dt} \sim \mathcal{N}(0, \sigma_\varepsilon^2)$. We condition the prior distribution on the training data resulting in the posterior mean m_+ and posterior variance σ_+^2 . For a given test input d_* , these are given by [6]

$$\begin{aligned} m_+(d_* | D^{dt}, Y^{dt}) &= k(d_*, D^{dt})(K(D^{dt}, D^{dt}) + \sigma_\varepsilon^2 I)^{-1} Y^{dt} \\ \sigma_+^2(d_* | D^{dt}, Y^{dt}) &= \\ &k(d_*, d_*) - k(d_*, D^{dt})(K(D^{dt}, D^{dt}) + \sigma_\varepsilon^2 I)^{-1} k(D^{dt}, d_*), \end{aligned}$$

for $k(d_*, D^{dt}) = (k(d_*, d_i))_{d_i \in D^{dt}} = k(D^{dt}, d_*)^\top$, with $k(d_*, D^{dt}) \in \mathbb{R}^{1 \times N}$, and $K(D^{dt}, D^{dt}) = (k(d_i, d_j))_{d_i, d_j \in D^{dt}}$ with $K(D^{dt}, D^{dt}) \in \mathbb{R}^{N \times N}$. The covariance function (and thus the posterior mean and the posterior variance) depends on some hyperparameters. Given the input D^{dt} and output data Y^{dt} , we optimize the hyperparameters by maximizing the log marginal likelihood, see, e.g., [6, Eq. (2.30)].

In this work, one objective is to approximate the state transition function $f : \mathbb{R}^n \times \mathbb{R}^m \rightarrow \mathbb{R}^n$ and the output map $h : \mathbb{R}^n \times \mathbb{R}^m \rightarrow \mathbb{R}^p$ by GPs. We consider nonlinear systems of the following form

$$x(t+1) = f(x(t), u(t)) + w(t) \quad (1a)$$

$$y(t) = h(x(t), u(t)) + v(t) \quad (1b)$$

with $x, w \in \mathbb{R}^n$, $u \in \mathbb{R}^m$, and $y, v \in \mathbb{R}^p$. Furthermore, we assume that the states and inputs evolve in compact sets, i.e., $x(t) \in \mathbb{X} \subset \mathbb{R}^n$ and $u(t) \in \mathbb{U} \subset \mathbb{R}^m$ and that the

functions f and h are continuous. As mentioned above, the objective is to approximate the functions f and h by GPs. To this end, i.e., only for modeling purposes, we assume w and v to be normally distributed. This setting has already been considered in various works in the area of GP-based estimation/control, see, e.g., [8], [10], [20]. Although the true process and measurement disturbances w and v , respectively, are typically bounded in real applications, they are considered to be normally distributed within the (GP) modeling framework. Note that the hyperparameter σ_ε , which corresponds to the measurement noise variance (see above), is tuned to get the best approximation of the unknown function, compare the discussion in [10, Sec. II-C].

In this work, we learn $n + p$ GPs to approximate the state-space model (1), i.e., one GP per component of the functions f and h , since GPs are typically defined for scalar outputs. Consequently, we denote the kernels associated to each component of the function f by k_{x_i} for $i = 1, \dots, n$ and the kernels associated to each component of the function h by k_{y_j} for $j = 1, \dots, p$. Furthermore, in our case, the regression input at time t corresponds to $d(t) = [x_1(t) \ \dots \ x_n(t) \ u_1(t) \ \dots \ u_m(t)]^\top$, i.e., the stacked state and control input at time t . The collected regression input data is stored in $D^{dt} = [d^{dt}(0) \ \dots \ d^{dt}(N-1)]$. Note that the individual GPs are not conditioned on the same regression output data. For instance, the GP approximating the first component of the state transition function f is conditioned on $X_1^{dt} := [x_1^{dt}(1) \ \dots \ x_1^{dt}(N)]^\top$ and the GP approximating the first component of h is conditioned on $Y_1^{dt} := [y_1^{dt}(0) \ \dots \ y_1^{dt}(N-1)]^\top$, where $x_i^{dt}(j)$ and $y_i^{dt}(j)$ denote the i -th component of the offline collected state and output at time j , respectively. To simplify the notation, we write

$$m_{+,x}(d(t)|D^{dt}, X^{dt}) := \begin{pmatrix} m_{+,x_1}(d(t)|D^{dt}, X_1^{dt}) \\ m_{+,x_2}(d(t)|D^{dt}, X_2^{dt}) \\ \vdots \\ m_{+,x_n}(d(t)|D^{dt}, X_n^{dt}) \end{pmatrix},$$

to denote the stacked vector of the posterior means approximating the components of f and, similarly, $m_{+,y}(d(t)|D^{dt}, Y^{dt})$ to denote the stacked vector of posterior means approximating the components of h . The learned system is defined as

$$x(t+1) = m_{+,x}(d(t)|D^{dt}, X^{dt}) + \tilde{w}(t) \quad (2a)$$

$$y(t) = m_{+,y}(d(t)|D^{dt}, Y^{dt}) + \tilde{v}(t) \quad (2b)$$

with $\tilde{w} \in \mathbb{R}^n$ and $\tilde{v} \in \mathbb{R}^p$. The original system dynamics (1) are obtained for

$$\tilde{w}(t) := f(x(t), u(t)) - m_{+,x}(d(t)|D^{dt}, X^{dt}) + w(t) \quad (3)$$

$$\tilde{v}(t) := h(x(t), u(t)) - m_{+,y}(d(t)|D^{dt}, Y^{dt}) + v(t). \quad (4)$$

In this work, we consider two different phases. First, we consider an offline phase, where we collect training data that is necessary to construct the posterior means and variances. In our case, the training data includes measurements of the inputs, outputs *and* states (as in many other works related

to data/learning-based state estimation such as, e.g., [12], [14], [21], [22]). In addition, we perform the hyperparameter optimization in this offline phase. Second, we consider an online phase in which only measurements of the inputs and outputs (but *not* the states) are available. To estimate the states in the online phase, we employ the GP-based MHE scheme that we introduce in Section III. The assumption that state measurements are available in an offline phase might be restrictive in general, but is certainly fulfilled in applications where one can measure all the states of the system using a dedicated laboratory and/or expensive hardware, compare the detailed discussion in [21], [22]. One concrete application where this setting is fulfilled is autonomous driving, where additional sensors can be installed in a vehicle to measure all the states (which then corresponds to the offline phase). However, to save costs, these sensors are not installed in a series production. Hence, the states must be estimated in the online phase [23], [24].

Remark 1: In the offline phase, we consider that the system states are affected by process noise, but not by measurement noise. That is, our state measurements are noise-free. This setting is commonly assumed in the literature [9], [12], [14], compare also [15, Rmk. 9]. In a more realistic setting, one would need to consider that the state measurements in the offline phase are corrupted by some measurement noise (*in addition* to the already here considered process noise), i.e., only $x_{\text{noisy}}(t) = x(t) + r(t)$ can be measured (with r being, e.g., some normally distributed noise). This more realistic setting leads to a substantially more involved regression problem (the offline regression inputs are only known up to some random noise, i.e., they are not known exactly), for which some initial results are available in [25], [26]. Nevertheless, if the noise affecting the regression inputs is small, the error made by assuming noise-free regression inputs is also small, compare [25, Fig. 5]. Hence, as a first approach, we consider noise-free regression inputs and leave the case of noisy regression inputs as an interesting subject for future work.

III. GP-BASED MHE SCHEME

In this section, we present the GP-based MHE scheme in detail. First, we present the optimization problem of the GP-based MHE scheme. Second, we explain the design of the weighting matrices in the cost function based on the posterior variances of the GPs.

A. Optimization Problem

At each time t , given the past $M_t = \min\{t, M\}$ (M being the horizon length) inputs $u(j)$ and measured outputs $y(j)$ for $j \in \mathbb{I}_{[t-M_t, t-1]}$, solve

$$\underset{\bar{x}(t-M_t|t), \bar{w}(\cdot|t)}{\text{minimize}} \quad J(\bar{x}(t-M_t|t), \bar{w}(\cdot|t), \bar{v}(\cdot|t), t) \quad (5a)$$

$$\text{s. t. } \bar{x}(j+1|t) = m_{+,x}(\bar{d}(j|t)|D^{dt}, X^{dt}) + \bar{w}(j|t), \quad (5b)$$

$$y(j) = m_{+,y}(\bar{d}(j|t)|D^{dt}, Y^{dt}) + \bar{v}(j|t), \quad (5c)$$

$$\forall j \in \mathbb{I}_{[t-M_t, t-1]}$$

$$\bar{x}(j|t) \in \mathbb{X} \quad \forall j \in \mathbb{I}_{[t-M_t, t]} \quad (5d)$$

with

$$\bar{d}(j|t) := [\bar{x}_1(j|t) \quad \dots \quad \bar{x}_n(j|t) \quad u_1(j) \quad \dots \quad u_m(j)]^\top$$

and

$$\begin{aligned} J(\bar{x}(t - M_t|t), \bar{w}(\cdot|t), \bar{v}(\cdot|t), t) \\ := 2\|\bar{x}(t - M_t|t) - \hat{x}(t - M_t)\|_{(\Sigma_{x, \bar{d}(t - M_t - 1|t - M_t)})^{-1}}^2 \eta^{M_t} \\ + \sum_{j=1}^{M_t} 2\eta^{j-1} \left(\|\bar{w}(t - j|t)\|_{(\Sigma_{y, \bar{d}(t-j|t)})^{-1}}^2 \right. \\ \left. + \|\bar{v}(t - j|t)\|_{(\Sigma_{y, \bar{d}(t-j|t)})^{-1}}^2 \right). \end{aligned} \quad (5e)$$

The GP-based MHE scheme is composed of a cost function (5a), (5e) and some constraints (5b) - (5d). By (5b) and (5c), we guarantee that the estimated state sequences satisfy the learned system dynamics given by the posterior means. The notation $\bar{x}(j|t)$ denotes the estimated state at time j , estimated at time t (and analogously for the estimated process noise and the estimated measurement noise denoted by \bar{w} and \bar{v} , respectively). The estimated process and measurement noise account for the noise in the online phase affecting the system *and* potential approximation errors of the functions f and h . Inherent system constraints, such as, e.g., nonnegativity constraints of chemical or hormone concentrations can be considered in (5d).

Remark 2: Note that many model-based MHE schemes additionally consider known constraints on the estimated process and measurement noise in order to improve the estimation performance. Here, the estimated process and measurement noise account for possible approximation errors of the functions f and h (in addition to the actual noise), which might not be available in practice. Nevertheless, if such knowledge of the approximation errors is available, constraints on \bar{w} and \bar{v} can also be included in the GP-based MHE scheme (5).

The cost function contains two parts. The first part is called prior weighting, which penalizes the difference between the initial element of the estimated state sequence $\bar{x}(t - M_t|t)$ and the estimated state $\hat{x}(t - M_t)$ that was estimated M_t steps in the past. The weighting matrix is chosen as $\Sigma_{x, \bar{d}(t - M_t - 1|t - M_t)}$, which we will explain in detail in the following subsection.

The second part is called stage cost, where we penalize the estimated process and measurement noise \bar{w} and \bar{v} , respectively. The weighting matrices $\Sigma_{x, \bar{d}(t-j|t)}$ and $\Sigma_{y, \bar{d}(t-j|t)}$ are also explained in detail in the following subsection, compare (6) and (7), respectively. We additionally consider a discount factor η which has a fading memory effect: the more a disturbance lies in the past, the less does it influence the cost function. In the context of MHE, discount factors have been introduced in [27] and proven to be very useful in robust stability proofs of different MHE schemes, compare, e.g., [28]–[30].

Once the optimization problem is solved, the optimal estimated state sequence is denoted by $\hat{x}(\cdot|t)$ (similarly, we denote the optimal process and measurement noise by \hat{w} and \hat{v} , respectively) and the estimated state at time t is set to $\hat{x}(t) := \hat{x}(t|t)$. The cost of the optimal trajectory is denoted by $J^* := J(\hat{x}(t - M_t|t), \hat{w}(\cdot|t), \hat{v}(\cdot|t), t)$.

B. Design of the Weighting Matrices

As mentioned in the introduction, the weighting matrices in our MHE scheme (5) are selected such that they quantify the uncertainty of the predicted regression outputs. We now explain how such a design is achieved. In MHE, we estimate a whole state trajectory of length $M + 1$. This estimation is based on M one-step-ahead predictions. Loosely speaking, this means that regression outputs at one time instant are used as regression inputs at the next time instant. Since the regression outputs are uncertain, we need to consider this uncertainty in the regression input at the next time instant. Ideally, we would like to propagate a normally distributed regression input through the GPs. However, it is impossible to *analytically* propagate uncertain regression inputs through nonlinear dynamics (as the GP-based state space model used in (5b) and (5c)) in the sense that we cannot compute the distribution of the regression outputs in closed form, compare [15, Sec. 2.3.2]. In the literature, two approaches have been proposed to handle this issue. The first one is called “moment matching”. The idea is to approximate the unknown distribution of the propagated input by a Gaussian distribution with the same mean and the same variance (i.e., the same moments) as the true distribution [31, Sec. 4.1]. This approach is computationally demanding. The second approach is to propagate the uncertainty by linearizing the posterior means (which is a similar approach as in the extended Kalman filter) [9], [12] [31, Sec. 4.2]. Since we here already combine an optimization-based state estimation method (MHE) with a learning technique (GP regression), which are both computationally expensive, we follow the second approach. Hence, when linearizing the posterior means, the weighting matrices (corresponding to the propagated uncertainties) are defined as (compare [9], [12] [31, Sec. 4.2])

$$\begin{aligned} \Sigma_{x, \bar{d}(t-j|t)} := \min \left\{ \Sigma_w + \Sigma_{x, \bar{d}(t-j|t)}^{\text{os}} \right. \\ \left. + A_{\bar{d}(t-j|t)} \Sigma_{x, \bar{d}(t-j-1|t)} A_{\bar{d}(t-j|t)}^\top, \Sigma_x^{\text{max}} \right\} \end{aligned} \quad (6)$$

$$\begin{aligned} \Sigma_{y, \bar{d}(t-j|t)} := \min \left\{ \Sigma_v + \Sigma_{y, \bar{d}(t-j|t)}^{\text{os}} \right. \\ \left. + C_{\bar{d}(t-j|t)} \Sigma_{y, \bar{d}(t-j-1|t)} C_{\bar{d}(t-j|t)}^\top, \Sigma_y^{\text{max}} \right\} \end{aligned} \quad (7)$$

for $j = 1, \dots, M_t$ and $\Sigma_x^{\text{max}} \succcurlyeq \Sigma_w \succ 0$ and $\Sigma_y^{\text{max}} \succcurlyeq \Sigma_v \succ 0$, where Σ_x^{max} and Σ_y^{max} are user-defined constant matrices, compare Remark 4 below. The first terms in (6) and (7) correspond to the diagonal matrices

$$\Sigma_w := \text{diag}(\sigma_{w_1}^2, \dots, \sigma_{w_n}^2) \quad (8)$$

$$\Sigma_v := \text{diag}(\sigma_{v_1}^2, \dots, \sigma_{v_p}^2) \quad (9)$$

where $\sigma_{w_1}^2, \dots, \sigma_{w_n}^2$ and $\sigma_{v_1}^2, \dots, \sigma_{v_p}^2$ are the noise variances in the online phase of each dimension of the functions f and h . The second term corresponds to the one-step-ahead uncertainties $\Sigma_{x, \bar{d}(t-j|t)}^{\text{os}}$ and $\Sigma_{y, \bar{d}(t-j|t)}^{\text{os}}$ defined as

$$\begin{aligned} \Sigma_{x, \bar{d}(t-j|t)}^{\text{os}} := \text{diag}(\sigma_{+, x_1}^2(\bar{d}(t-j|t)|D^{dt}, X_1^{dt}), \dots, \\ \sigma_{+, x_n}^2(\bar{d}(t-j|t)|D^{dt}, X_n^{dt})) \end{aligned} \quad (10)$$

$$\begin{aligned} \Sigma_{y, \bar{d}(t-j|t)}^{\text{os}} := \text{diag}(\sigma_{+, y_1}^2(\bar{d}(t-j|t)|D^{dt}, Y_1^{dt}), \dots, \\ \sigma_{+, y_p}^2(\bar{d}(t-j|t)|D^{dt}, Y_p^{dt})). \end{aligned} \quad (11)$$

Finally, the third term in (6) and (7) corresponds to the propagated uncertainties, i.e., accounts for the fact that the (online) regression inputs are uncertain, where

$$A_{\bar{d}(t-j|t)} := \frac{\partial m_{+,x}((x, u)|D^{dt}, X^{dt})}{\partial x} \Big|_{\bar{d}(t-j|t)} \quad (12)$$

and

$$C_{\bar{d}(t-j|t)} := \frac{\partial m_{+,y}((x, u)|D^{dt}, X^{dt})}{\partial x} \Big|_{\bar{d}(t-j|t)}, \quad (13)$$

stand for the linearized posterior means. The matrices $\Sigma_{x,\bar{d}(t-j-1|t)}$ and $\Sigma_{y,\bar{d}(t-j-1|t)}$ represent the uncertainties from the previous time instant. Note that the indices of the weighting matrices in (6) - (7) correspond to the regression input. For instance, the uncertainty $\Sigma_{x,\bar{d}(t-j|t)}$ quantifies the uncertainty of our approximation of $\bar{x}(t-j+1|t)$. Furthermore, in the third term of (7), we consider $\Sigma_{x,\bar{d}(t-j-1|t)}$, but not $\Sigma_{y,\bar{d}(t-j-1|t)}$. This is because the uncertainty in the predictions of the (physical) output does not depend on previous regression outputs. The uncertainty $\Sigma_{x,\bar{d}(t-M_i-1|t)}$ is set to zero, because the initial element of the estimated trajectory is not obtained by propagating an uncertain regression input through a GP.

Note that the final weighting matrices in (6) - (7) are set to the minimum of the sum described above and some (user defined) maximal uncertainties Σ_x^{\max} and Σ_y^{\max} . These maximal uncertainties are needed for technical reasons to prove robust stability of the GP-based MHE scheme, compare also Remark 4 at end of Subsection IV-A. Moreover, in the proof of Theorem 1, we consider the cost, when the real (unknown) system trajectory is considered within the optimization problem. In this case, we denote the uncertainty of the predicted regression outputs related to the regression input at time $t-j$ by $\Sigma_{x,d(t-j)}$ and $\Sigma_{y,d(t-j)}$ (and we refer the reader to Footnote 1 below concerning the initialization of these uncertainties).

The effect of the weighting matrices (6) - (7) is the following: if a small (large) amount of training data is available, the uncertainty in the predictions is rather large (small). Since we consider the inverse of the uncertainty in the cost function, the induced weight on \bar{w} and \bar{v} is small (large). A small (large) weight implies that we allow for large (small) values of the estimated process and measurement noise to reconstruct the measured outputs. This is meaningful since the posterior mean will be a poor (good) approximation of the true unknown function. Thus, the weights in the cost function (5e) are adapted according to the quality of the GP approximations. The benefit of using this choice of cost function will also be illustrated in Section VI.

The uncertainty propagation is not only useful to account for the uncertainties in the predicted trajectories, but also serves as a natural choice for the weighting matrix in the prior weighting. By propagating the uncertainty in the described manner, we obtain an estimate of the uncertainty related to the current state estimate $\hat{x}(t)$, i.e., $\Sigma_{x,\bar{d}(t-1|t)}$. Note that this state estimate becomes the prior M time instants later and hence, the uncertainty of this prior is $\Sigma_{x,\bar{d}(t-M_i-1|t-M_i)}$ (which is used as weighting matrix in the prior weighting). Once again,

if there is a large (small) uncertainty in the prior estimate, the induced weight is small (large), since we consider the inverse in the prior weighting of the cost function (5e). As long as $t < M$ (i.e., as long as not enough measurements are available to fill a complete horizon), a prior uncertainty $\Sigma_{x,\bar{d}(-1|0)}$ must be set by the user, similar to other nonlinear state estimation techniques as the extended Kalman filter.

IV. ROBUST STABILITY ANALYSIS

After having introduced the GP-based MHE scheme, we now analyze its robust stability properties.

A. Main result

We here use the following definition of practical robust exponential stability.

Definition 1: A state estimator for system (1) is practically robustly exponentially stable (pRES) if there exist scalars $C_1, C_2, C_3 > 0$, $\lambda_1, \lambda_2, \lambda_3 \in [0, 1)$, and $\alpha > 0$ such that the resulting state estimates $\hat{x}(t)$ satisfy

$$\|x(t) - \hat{x}(t)\| \leq \max \left\{ C_1 \|x(0) - \hat{x}(0)\| \lambda_1^t, \max_{j \in \mathbb{I}_{[0, t-1]}} C_2 \|w(j)\| \lambda_2^{t-j-1}, \max_{j \in \mathbb{I}_{[0, t-1]}} C_3 \|v(j)\| \lambda_3^{t-j-1}, \alpha \right\} \quad (14)$$

for all $t \in \mathbb{I}_{\geq 0}$, all initial conditions $x(0), \hat{x}(0) \in \mathbb{X}$, and every trajectory $(x(t), u(t), w(t), v(t))_{t=0}^{\infty}$ satisfying the system dynamics (1).

This definition states that the state estimation error is bounded at each time t by (i) the initial state estimation error, (ii) the real process and measurement noise, and (iii) a positive constant α . In this work, the introduction of the additional constant α is used to capture the effect of potential approximation errors on the state estimates.

To prove robust stability, we introduce the constant matrices Σ_x^{\min} and Σ_y^{\min} that satisfy

$$(\Sigma_x^{\max})^{-1} \leq (\Sigma_{x,\bar{d}(t-j|t)})^{-1} \leq (\Sigma_x^{\min})^{-1} \quad (15)$$

$$(\Sigma_y^{\max})^{-1} \leq (\Sigma_{y,\bar{d}(t-j|t)})^{-1} \leq (\Sigma_y^{\min})^{-1}. \quad (16)$$

for all $t \in \mathbb{I}_{\geq 0}$ and all $j = 1, \dots, M$ with Σ_x^{\max} and Σ_y^{\max} from (6) and (7), respectively. The matrices Σ_x^{\min} and Σ_y^{\min} can be set to the minimal possible uncertainties, which are $\Sigma_x^{\min} := \Sigma_w$ and $\Sigma_y^{\min} := \Sigma_v$ with Σ_w and Σ_v as in (8) and (9), respectively.

To prove robust stability of the GP-based MHE scheme (5), we need that the learned system (2) satisfies a nonlinear detectability notion called incremental input/output-to-state stability (δ -IOSS). This notion (or similar versions of it) has been frequently used in the MHE literature to prove robust stability of various MHE schemes, see, e.g., [2], [27], [28]. Here, we assume that the learned system (2) admits a (quadratically bounded) δ -IOSS Lyapunov function, which is equivalent to the learned system being (exponentially) δ -IOSS [32] [3].

Assumption 1: The system (2) admits a δ -IOSS Lyapunov function $W_\delta : \mathbb{R}^n \times \mathbb{R}^n \rightarrow \mathbb{R}_{\geq 0}$ with quadratic bounds and

supply rate, i.e., there exist $\eta \in [0, 1)$, $P_1, P_2 \succ 0$, $\tilde{Q}, \tilde{R} \succ 0$ such that

$$\|x - \tilde{x}\|_{P_1}^2 \leq W_\delta(x, \tilde{x}) \leq \|x - \tilde{x}\|_{P_2}^2, \quad (17a)$$

$$\begin{aligned} & W_\delta\left(m_{+,x}(d|D^{dt}, X^{dt}) + \tilde{w}, m_{+,x}(\tilde{d}|D^{dt}, X^{dt}) + \tilde{w}'\right) \\ & \leq \eta W_\delta(x, \tilde{x}) + \|\tilde{w} - \tilde{w}'\|_{\tilde{Q}}^2 \\ & + \|m_{+,y}(d|D^{dt}, Y^{dt}) - m_{+,y}(\tilde{d}|D^{dt}, Y^{dt})\|_{\tilde{R}}^2 \end{aligned} \quad (17b)$$

for all $(x, u, \tilde{w}), (\tilde{x}, u, \tilde{w}')$ with $x, \tilde{x} \in \mathbb{X}$, $u \in \mathbb{U}$, where $d = [x_1 \ \dots \ x_n \ u_1 \ \dots \ u_m]^\top$, $\tilde{d} = [\tilde{x}_1 \ \dots \ \tilde{x}_n \ u_1 \ \dots \ u_m]^\top$.

The computation of a δ -IOSS Lyapunov function, i.e., the verification of Assumption 1, can be done via LMI conditions using, e.g., the methods proposed in [3, Sec. IV] or [30]. To simplify the notation, we introduce the following constants

$$\alpha_1^{\max} := \max_{x \in \mathbb{X}, u \in \mathbb{U}} \left\{ \|f(x, u) - m_{+,x}(d|D^{dt}, X^{dt})\|_{(\Sigma_x^{\min})^{-1}} \right\} \quad (18)$$

$$\alpha_2^{\max} := \max_{x \in \mathbb{X}, u \in \mathbb{U}} \left\{ \|h(x, u) - m_{+,y}(d|D^{dt}, Y^{dt})\|_{(\Sigma_y^{\min})^{-1}} \right\} \quad (19)$$

and $\alpha^{\max} := \max\{\alpha_1^{\max}, \alpha_2^{\max}\}$. These constants exist, since we assume that (i) the states and inputs evolve in compact sets, (ii) the functions f and h are continuous, and (iii) since the here considered squared exponential kernel leads to a continuous posterior mean. We are now ready to state the main result in this section.

Theorem 1: Let Assumption 1 hold with $P_1 = (\Sigma_x^{\max} + \varepsilon I)^{-1}$ (for some $\varepsilon \geq 0$), $P_2 = (\Sigma_x^{\max})^{-1}$, $\tilde{Q} = (\Sigma_x^{\max})^{-1}$ and $\tilde{R} = (\Sigma_y^{\max})^{-1}$ for Σ_x^{\max} and Σ_y^{\max} from (6) and (7), respectively. Then, there exist $\mu \in [0, 1)$ and a minimal horizon length \bar{M} such that for all $M \in \mathbb{I}_{\geq \bar{M}}$, the state estimation error of the GP-based MHE scheme (5) is bounded for all $t \in \mathbb{I}_{\geq 0}$ by¹

$$\begin{aligned} & \|\hat{x}(t) - x(t)\|_{(\Sigma_x^{\max} + \varepsilon I)^{-1}} \\ & \leq \max \left\{ 6\sqrt{\mu^t} \|\hat{x}(0) - x(0)\|_{(\Sigma_{x, \hat{d}(-1|0)})^{-1}}, \right. \\ & \max_{q \in \mathbb{I}_{[0, t-1]}} \left\{ \frac{12}{1 - \sqrt[4]{\mu}} \sqrt[4]{\mu^q} \|w(t-q-1)\|_{(\Sigma_{x, d(t-q-1)})^{-1}} \right\}, \\ & \max_{q \in \mathbb{I}_{[0, t-1]}} \left\{ \frac{12}{1 - \sqrt[4]{\mu}} \sqrt[4]{\mu^q} \|v(t-q-1)\|_{(\Sigma_{y, d(t-q-1)})^{-1}} \right\}, \\ & \left. \frac{12}{1 - \sqrt[4]{\mu}} \alpha^{\max} \right\}, \end{aligned} \quad (20)$$

Consequently, the GP-based MHE (5) is pRES according to Definition 1.

¹In the proof, we recursively iterate a contraction over M steps, as explained below (45). Note that the initial uncertainty at the beginning of each interval is set to zero, compare the paragraph below (13). For instance, the interval from $\Sigma_{x, d(t-1)}$ to $\Sigma_{x, d(t-M)}$ is initialized with $\Sigma_{x, d(t-M-1)} = 0$ and the interval from $\Sigma_{x, d(t-M-1)}$ to $\Sigma_{x, d(t-2M)}$ with $\Sigma_{x, d(t-2M-1)} = 0$. In general, the weighing matrix $\Sigma_{x, d(t-q-1)}$ is initialized with $\Sigma_{x, d(t-[q/M] \times M-1)} = 0$. With slight abuse of notation, we do not specify this initialization to improve the readability of the proof.

The proof of Theorem 1 is given in Appendix A. It is constructive in the sense that an explicit estimate for the minimal required horizon length \bar{M} is obtained (compare (43)).

Theorem 1 guarantees that the state estimation error is bounded for any time instant $t \in \mathbb{I}_{\geq 0}$ in dependence of (i) the initial state estimation error, (ii) the true process and measurement noise, (iii) and the maximal difference between the true functions f and h and their approximating posterior means. This bound is less conservative than the bound obtained in the preliminary conference version of this work [19], since the weights on the norm of w and v do not correspond to the inverse of the minimal possible uncertainty, but to the uncertainty related to the true system trajectory.

Remark 3: Here, we comment on the case of having a larger amount of training data available. On the one hand, more training data in general decreases the uncertainty matrices $\Sigma_{x, d(t-q-1)}$ and $\Sigma_{y, d(t-q-1)}$ and hence also a smaller value of the maximum uncertainty Σ_x^{\max} can be chosen in (6), compare Remark 4 below. If these additional data points are very informative (i.e., are from the region with the highest uncertainty), then the decrease of Σ_x^{\max} will be larger than the one of the variable matrices $\Sigma_{x, d(t-q-1)}$ and $\Sigma_{y, d(t-q-1)}$, which results in a better bound (20). On the other hand, if the new data is less informative in the sense that the maximum uncertainty Σ_x^{\max} can only be slightly decreased, then this might not result in an improved (or even worse) error bound (20). The reason for this latter (slightly counter-intuitive) observation lies in the proof technique. We bound a (manipulated) expression based on the dissipation inequality (17b) of the δ -IOSS Lyapunov function with the cost function, compare inequality (39) in Appendix A. In the cost function, a larger weight in case of small uncertainties is meaningful, compare the reasoning at the end of Section III. However, this is not the case for the final state estimation error bounds. To avoid this effect, one can overapproximate the right-hand side of (20), by using the maximal possible weights $(\Sigma_x^{\min})^{-1}$ and $(\Sigma_y^{\min})^{-1}$ as weights of w and v , respectively. Note that this more conservative bound for the right hand side of (20) is independent of the number of training data, which means that the resulting bound (20) now can only improve with more training data (due to the fact that Σ_x^{\max} decreases).

Remark 4: In (6) and (7), we introduced the maximal uncertainties Σ_x^{\max} and Σ_y^{\max} , that are needed for technical reasons in the proof² of Theorem 1. These uncertainties need to be fixed a priori. The choice of the maximal uncertainties is a trade-off: If the maximal weighting matrices are set to large values, then one obtains more conservative error bounds (20) (since we consider the inverse of the maximal uncertainty Σ_x^{\max} on the left-hand side of (20)). In turn, if the maximal weighting matrices in (6) and (7) are set to rather small values, the weighting matrices will often correspond to these constant weighting matrices (which means that we do not fully exploit the inherent uncertainty quantification of the GPs in the cost function).

²If we did not consider such a maximal uncertainty, the maximal propagated uncertainty would depend on the horizon length M (due to the first term in (6) and (7)), meaning that it is not guaranteed that one can always find an M large enough such that $\mu^M \in [0, 1)$ holds with μ^M from (43).

B. Application of GP uniform error bounds

So far, the error bound in Theorem 1 depends on the maximal approximation error, captured by the constant α^{\max} . The dependency on the maximal approximation error can be avoided by considering a slightly different MHE scheme and uniform error bounds for GPs. These error bounds typically bound (probabilistically) the norm of the difference between some true function and the related posterior mean [20], [33]–[35]. Typically, the upper bound consists of a constant multiplied by the posterior variance.

These bounds were developed for GPs with a single output. If we learn multiple (independent) GPs for the different components of the functions f and h and by considering deterministic regression inputs, we can apply the GP uniform error bounds separately for each component. However, due to the here considered uncertain regression inputs, there can be a non-zero covariance between the scalar GPs for each component. Hence, we cannot apply these bounds directly. However, this can be avoided when considering deterministic regression inputs (hence, not accounting for the propagated uncertainties, only for the one-step-ahead uncertainties) and the following cost function

$$\begin{aligned} J(\bar{x}(t-M_t|t), \bar{w}(\cdot|t), \bar{v}(\cdot|t), t) \\ := 2\|\bar{x}(t-M_t|t) - \hat{x}(t-M_t)\|_{(\tilde{\Sigma}_{x,\bar{d}(t-M_t-1|t-M_t)})^{-1}}^2 \eta^{M_t} \\ + \sum_{j=1}^{M_t} 2\eta^{j-1} \left(\|\bar{w}(t-j|t)\|_{(\tilde{\Sigma}_{x,\bar{d}(t-j|t)})^{-1}}^2 \right. \\ \left. + \|\bar{v}(t-j|t)\|_{(\tilde{\Sigma}_{y,\bar{d}(t-j|t)})^{-1}}^2 \right). \end{aligned} \quad (21)$$

for

$$\tilde{\Sigma}_{x,\bar{d}(t-j|t)} := \Sigma_w + \Sigma_{x,\bar{d}(t-j|t)}^{\text{os}} \quad (22)$$

$$\tilde{\Sigma}_{y,\bar{d}(t-j|t)} := \Sigma_v + \Sigma_{y,\bar{d}(t-j|t)}^{\text{os}}. \quad (23)$$

and $\tilde{\Sigma}_{x,\bar{d}(t-M_t-1|t-M_t)}$ defined as $\Sigma_{x,\bar{d}(t-M_t-1|t-M_t)}$. Compared to (6) and (7), we now do not consider the propagated uncertainties and hence only have a rough estimate of the uncertainty within the estimated trajectories. Once again, we assume the existence of some matrices $\tilde{\Sigma}_x^{\max}$, $\tilde{\Sigma}_x^{\min}$, $\tilde{\Sigma}_y^{\max}$, and $\tilde{\Sigma}_y^{\min}$ such that

$$(\tilde{\Sigma}_x^{\max})^{-1} \leq (\tilde{\Sigma}_{x,\bar{d}(t-j|t)})^{-1} \leq (\tilde{\Sigma}_x^{\min})^{-1} \quad (24)$$

$$(\tilde{\Sigma}_y^{\max})^{-1} \leq (\tilde{\Sigma}_{y,\bar{d}(t-j|t)})^{-1} \leq (\tilde{\Sigma}_y^{\min})^{-1} \quad (25)$$

for all $t \in \mathbb{I}_{\geq 0}$ and all $j = 1, \dots, M$. In fact, for the cost function (21) - (23) a lower bound for $\tilde{\Sigma}_x^{\min}$ is given by $\tilde{\Sigma}_x^{\min} := \Sigma_w$ and an upper bound for $\tilde{\Sigma}_x^{\max}$ by $\tilde{\Sigma}_x^{\max} := \text{diag}(\sigma_{f,x_1}^2, \dots, \sigma_{f,x_n}^2) + \Sigma_w$ (where σ_{f,x_i}^2 denotes the signal variance of the squared exponential kernel) and similarly for $\tilde{\Sigma}_y^{\max}$ and $\tilde{\Sigma}_y^{\min}$. Considering this setting, we can apply the GP error bounds to obtain probabilistic stability guarantees independent of some maximal approximation error (as captured by α^{\max} in the previous subsection).

There are two different approaches to develop GP uniform error bounds. The first approach assumes that the unknown function is a sample from a Gaussian process and that the noise affecting the function outputs is Gaussian (Bayesian approach)

[20], [33]. In the second approach, the main assumptions are that the unknown function belongs to the reproducing kernel Hilbert space (RKHS)³ that is generated by the covariance function and that the corresponding norm of the unknown function is bounded (frequentist approach) [33]–[35]. On one side, the advantage of the Bayesian approach is that the space of functions for which the bounds hold is large. On the other side, the advantage of the frequentist approach is that the noise must not necessarily be Gaussian and can also be sub-Gaussian, as defined below.

Definition 2: The random variable ξ is said to be R -sub-Gaussian [34, Sec. 2] for a fixed constant $R \geq 0$, if

$$\mathbb{E}(e^{\lambda\xi}) \leq e^{\frac{R^2\lambda^2}{2}} \quad (26)$$

holds for all $\lambda \in \mathbb{R}$.

Note that noise distributions bounded in $[-R, R]$ satisfy this definition [34].

We follow the frequentist approach, since it allows to bound the regression error for larger classes of noise. Consequently, we need the following assumption.

Assumption 2: Each component of the unknown functions f and h is a function from the RKHS⁴ of the kernel used to approximate this component, i.e., $f_i \in \mathcal{H}_{k_{x_i}}$ and $h_j \in \mathcal{H}_{k_{y_j}}$ for all $i = 1, \dots, n$ and $j = 1, \dots, p$. Furthermore, there exist constants B_{x_i} and B_{y_j} such that f_i and h_j satisfy $\|f_i\|_{k_{x_i}} \leq B_{x_i}$ and $\|h_j\|_{k_{y_j}} \leq B_{y_j}$ for all $i = 1, \dots, n$ and $j = 1, \dots, p$. The noise affecting the regression output measurements is R -sub-Gaussian.

To simplify the notation, we define

$$\begin{aligned} \Delta^x &:= \sqrt{\lambda_{\max}((\tilde{\Sigma}_x^{\min})^{-1})} \\ &\times \sum_{i=1}^n \max_{x \in \mathbb{X}, u \in \mathbb{U}} \left\{ B_{x_i} \sigma_{+,x_i}(d|D^d, X_i^d) + \eta_{N,x_i}(d) \right\} \end{aligned} \quad (27)$$

$$\begin{aligned} \Delta^y &:= \sqrt{\lambda_{\max}((\tilde{\Sigma}_y^{\min})^{-1})} \\ &\times \sum_{j=1}^p \max_{x \in \mathbb{X}, u \in \mathbb{U}} \left\{ B_{y_j} \sigma_{+,y_j}(d|D^d, Y_j^d) + \eta_{N,y_j}(d) \right\} \end{aligned} \quad (28)$$

where

$$\begin{aligned} \eta_{N,x_i}(d) &:= R \|(K_{x_i}(D^d, D^d) + \sigma_{w_i}^2 I_N)^{-1} k_{x_i}(d, D^d)\| \\ &\times \sqrt{N + 2\sqrt{N} \sqrt{\log(1/\delta)} + 2 \log(1/\delta)} \end{aligned} \quad (29)$$

$$\begin{aligned} \eta_{N,y_j}(d) &:= R \|(K_{y_j}(D^d, D^d) + \sigma_{v_j}^2 I_N)^{-1} k_{y_j}(d, D^d)\| \\ &\times \sqrt{N + 2\sqrt{N} \sqrt{\log(1/\delta)} + 2 \log(1/\delta)} \end{aligned} \quad (30)$$

for $i = 1, \dots, n$ and $j = 1, \dots, p$ with $\delta > 0$. Additionally, we define $\Delta^{\max} := \max\{\Delta^x, \Delta^y\}$.

Corollary 1: Let Assumptions 1 (with $P_1 = (\tilde{\Sigma}_x^{\max} + \tilde{\varepsilon}I)^{-1}$, $P_2 = (\tilde{\Sigma}_x^{\max})^{-1}$, $\tilde{Q} = (\tilde{\Sigma}_x^{\max})^{-1}$ and $\tilde{R} = (\tilde{\Sigma}_y^{\max})^{-1}$ for some $\tilde{\varepsilon} \geq 0$ as well as $\tilde{\Sigma}_x^{\max}$ and $\tilde{\Sigma}_y^{\max}$ from (24) and (25),

³Introductions to the RKHS can be found in [36, Ch. 4] and [37, Sec. 2.1.5].

⁴We denote the RKHS of the kernel k by \mathcal{H}_k and the corresponding norm by $\|\cdot\|_k$.

respectively⁵) and 2 hold. Then, there exist $\mu \in [0, 1)$ and a minimal horizon length \bar{M} such that for all $M \in \mathbb{I}_{\geq \bar{M}}$ the state estimation error for the GP-based MHE scheme (5) with (5e) replaced by (21) is bounded by

$$P \left(\left\| \hat{x}(t) - x(t) \right\|_{(\bar{\Sigma}_x^{\max + \varepsilon I})^{-1}} \leq \max \left\{ 6\sqrt{\mu}^t \left\| \hat{x}(0) - x(0) \right\|_{(\bar{\Sigma}_{x, \hat{d}(-1|0)})^{-1}}, \right. \right. \\ \left. \max_{q \in \mathbb{I}_{[0, t-1]}} \left\{ \frac{12}{1 - \sqrt[4]{\mu}} \sqrt[4]{\mu}^q \left\| w(t-q-1) \right\|_{(\bar{\Sigma}_{x, d(t-q-1)})^{-1}} \right\}, \right. \\ \left. \max_{q \in \mathbb{I}_{[0, t-1]}} \left\{ \frac{12}{1 - \sqrt[4]{\mu}} \sqrt[4]{\mu}^q \left\| v(t-q-1) \right\|_{(\bar{\Sigma}_{y, d(t-q-1)})^{-1}} \right\}, \right. \\ \left. \frac{12}{1 - \sqrt[4]{\mu}} \Delta^{\max} \right\} \geq 1 - (n+p)\delta. \quad (31)$$

The proof of Corollary 1 is given in Appendix B. The key idea of the proof is to bound probabilistically the norm of the difference between the true function components and the posterior means by applying [35, Prop. 2]. Consequently, the final state estimation error bounds are probabilistic in nature.

V. DETECTABILITY ANALYSIS

After having presented the GP-based MHE scheme, we address an important question regarding the use of a learning-based model as in (2) in a state estimation framework. Assumption 1, required in our main theoretical results above, states that the learned system (2) is detectable in the sense that it admits a δ -IOSS Lyapunov function. Clearly, if the model (2) is not detectable, then its use for state estimation is not justified. Thus, it is of our interest to determine the conditions under which the learned model (2) preserves the detectability property of the true system (1). Although we have focused so far on the use of GPs for function approximation, the results of this section are applicable if the state transition function f and the output map h are approximated by using any machine learning technique. Furthermore, we consider δ -IOSS as nonlinear detectability notion in its general form, as defined below.

Definition 3: A function $W_\delta : \mathbb{R}^n \times \mathbb{R}^n \rightarrow \mathbb{R}_{\geq 0}$ is a δ -IOSS Lyapunov function for system (1) if there exist $\alpha_1, \alpha_2 \in \mathcal{K}_\infty$, $\sigma_w, \sigma_h \in \mathcal{K}$, and $\eta \in [0, 1)$ such that

$$\alpha_1(\|x - \tilde{x}\|) \leq W_\delta(x, \tilde{x}) \leq \alpha_2(\|x - \tilde{x}\|), \quad (32a)$$

$$W_\delta(f(x, u) + w, f(\tilde{x}, u) + \tilde{w}) \\ \leq \eta W_\delta(x, \tilde{x}) + \sigma_w(\|w - \tilde{w}\|) + \sigma_h(\|h(x, u) - h(\tilde{x}, u)\|), \quad (32b)$$

for all $x, \tilde{x} \in \mathbb{X}$, $u \in \mathbb{U}$, and $w, \tilde{w} \in \mathbb{W} \subseteq \mathbb{R}^n$.

As mentioned above, we assume in this section that the considered unknown system is detectable in the sense that a δ -IOSS Lyapunov function exists.

⁵Here we use different weights in the Lyapunov function W_δ to simplify some steps in the proof. Note that the Lyapunov function W_δ can be scaled meaning that the weights used here do not change the detectability assumption, compare [3, Rmk. 1].

Assumption 3: System (1) admits a δ -IOSS Lyapunov function according to Definition 3.

Moreover, we define the approximation errors

$$e_x(x, u) := f(x, u) - m_{+,x}((x, u)|D^{dt}, X^{dt}) \quad (33)$$

$$e_y(x, u) := h(x, u) - m_{+,y}((x, u)|D^{dt}, Y^{dt}) \quad (34)$$

with f, h from (1) and $m_{+,x}, m_{+,y}$ from (2). We introduce the following additional assumption.

Assumption 4: Consider systems (1) and (2), and Definition 3. Let $\tilde{\eta}$ be such that $0 \leq \eta \leq \tilde{\eta} < 1$. The following inequality

$$\sigma_w(2\|e_x(x, u) - e_x(\tilde{x}, u)\|) \\ + \sigma_h(2\|e_y(x, u) - e_y(\tilde{x}, u)\|) \leq (\tilde{\eta} - \eta)W_\delta(x, \tilde{x}) \quad (35)$$

holds for all $x, \tilde{x} \in \mathbb{X}$, $u \in \mathbb{U}$.

The left-hand side of the inequality corresponds to the sum of two \mathcal{K} functions, where the arguments are the norms of the difference of the state and output approximation errors at the points x and \tilde{x} . This inequality will be needed in Theorem 2 below and quantifies how large the approximation error can be such that detectability of the learned system is still guaranteed. In particular, for larger approximation errors e_x and e_y , a larger constant $\tilde{\eta}$ will be required. Note that if the model is learned exactly, i.e., $f \equiv m_x$ and $h \equiv m_y$ (from (1) and (2)), the left-hand side of Assumption 4 equals zero, meaning that we can choose $\tilde{\eta} = \eta$.

Moreover, we introduce the set

$$\mathbb{E}_x := \left\{ e \in \mathbb{R}^n \mid e = m_{+,x}((x, u)|D^{dt}, Y^{dt}) - f(x, u), \right. \\ \left. x \in \mathbb{X}, u \in \mathbb{U} \right\} \quad (36)$$

and assume the following.

Assumption 5: Consider the set \mathbb{E}_x as defined in (36) and the set \mathbb{W} from Definition 3. These sets satisfy $\mathbb{E}_x \subset \mathbb{W}$.

This assumption is required in the following theorem to guarantee that the set \mathbb{W} (composed of disturbances w such that there exists a δ -IOSS Lyapunov function as in Definition 3) captures possible approximation errors. We now state the main result of this section.

Theorem 2: Let Assumptions 3, 4, and 5 hold and consider $w \in \mathbb{W} \ominus \mathbb{E}_x$. Then, the learned system (2) admits a δ -IOSS Lyapunov function.

The proof of Theorem 2 is given in Appendix C.

Intuitively, this theorem states that we do not lose detectability, when approximating the system dynamics as long as Assumptions 4 - 5 are satisfied. The proof proceeds by establishing the bounds (32) for the learned system (2), but with the in general larger discount factor $\tilde{\eta}$ instead of η in (32b). This is to be expected, since the approximation error needs to be compensated. Moreover, the set to which the disturbances w can belong according to Theorem 2 is smaller for the learned system dynamics compared to the true dynamics (in order to admit a δ -IOSS Lyapunov function), which is also due to the fact that we need to account for the approximation errors.

It is worth mentioning that Theorem 2 does not make use of the properties of GPs. Hence, it is a general result and also

holds for other approximating techniques such as, e.g., neural networks. Moreover, here we use the general definition of a δ -IOSS Lyapunov function. In case the true system satisfies the stronger property of exponential δ -IOSS [3], a similar result can be derived.

We close this section by noting that the practical application of this theorem is, in general, limited, due to the fact that Assumptions 4 and 5 are hard to verify. In general, the state transition function and the output map are unknown and hence the approximation errors (33) - (34) cannot be computed analytically. Hence, the theorem must be interpreted as an existence result, showing that if the true (unknown) system is detectable, then the learned system preserves this property if the approximation error is small enough. Finally, as already discussed above, in practice a direct computation of a δ -IOSS Lyapunov function for the learned system can be done by the methods introduced in [3, Sec. IV] [30].

VI. APPLICATION TO BATCH REACTOR

In this section, we illustrate the performance of the GP-based MHE scheme⁶. The scheme is implemented using the software Casadi [38] and the nonlinear program solver IPOPT [39]. We consider the following Euler-discretized system

$$\begin{aligned} x_1(t+1) &= x_1(t) + T(-2k_1x_1^2(t) + 2k_2x_2(t)) + w_1(t) \\ x_2(t+1) &= x_2(t) + T(k_1x_1^2(t) - k_2x_2(t)) + w_2(t) \\ y(t) &= x_1(t) + x_2(t) + v(t) \end{aligned} \quad (37)$$

with sampling time $T = 0.1$, constants $k_1 = 0.16$, $k_2 = 0.0064$ which corresponds to a batch reactor system [1, Ch. 4], [40]. This system is a benchmark example in the MHE literature, since other nonlinear state estimation techniques, such as the extended Kalman filter or the unscented Kalman filter, can fail to converge or produce physically implausible state estimates, compare [1].

A. GP-based MHE scheme

As mentioned in Section II, we here consider two different phases. In the offline phase, we assume to have measurements of input/output/state trajectories available. This data is generated by simulating 31 time steps for three different initial conditions ($x_{0,1} = (3 \ 1)^\top$, $x_{0,2} = (1 \ 3)^\top$, and $x_{0,3} = (2 \ 4)^\top$) and normally distributed noise with mean $\mu_w = 0$ and variance $\Sigma_w = 10^{-5}I_n$ (concerning the process noise affecting the states) and $\mu_v = 0$ and $\Sigma_v = 10^{-3}I_p$ (concerning the noise affecting the output measurements). Using this dataset, we optimize the hyperparameters by maximizing the log marginal likelihood. Then, we switch to the online phase and apply the GP-based MHE scheme (5). We consider $M = 15$, $\eta = 0.91$, $\hat{x}(0) = (0.1 \ 4.5)^\top$, $x(0) = (2 \ 2)^\top$ and normally distributed measurement noise with mean $\mu_v = 0$ and variance $\Sigma_v = 10^{-3}I_p$, as well as normally distributed process noise with mean $\mu_w = 0$ and variance $\Sigma_w = 10^{-5}I_n$. The initial weighting matrix of the prior is

selected as $\Sigma_{\hat{d}(-1|0)} = P^{-1}$ where P is the prior matrix from [3, Sec. V. A] and the maximal uncertainties are chosen as $\Sigma_x^{\max} = \text{diag}(10^5, 10^5)$ and $\Sigma_y^{\max} = 10^5$. We know that the states evolve in a compact set $\mathbb{X} = \{x \in \mathbb{R}^2 | 0.1 \leq x_i \leq 4.5, i = \{1, 2\}\}$. We implement the weighting matrices (6) and (7) by computing an upper bound of the maximal eigenvalue of the propagated uncertainty (which can be done by using Gershgorin's circle theorem). Alternatively, one could compute the eigenvalues symbolically, which however only works for square matrices of dimensions three (or less) in Casadi. In the simulation example, we observed that the upper bound of the propagated uncertainty, i.e., the Σ_x^{\max} was never used. Hence, for practical application, one could also omit the implementation of the min operation and only consider the first term in (6) and (7). The results of the GP-based MHE scheme are illustrated in the last panel of Figure 1 called "GP full". As guaranteed by Theorem 1, the GP-based MHE scheme is pRES.

Remark 5: In [3], (LMI-based) sufficient conditions have been introduced to guarantee the existence of a δ -IOSS Lyapunov function (implying that the underlying system is δ -IOSS). These conditions are based on the differential dynamics of the system and can also be used in this work. We consider Σ_x^{\max} and Σ_y^{\max} as specified above. We were able to verify Assumption 1 for $\{x \in \mathbb{R}^2 | 0.5 \leq x_i \leq 4.5, i = \{1, 2\}\}$. The minimal horizon length \bar{M} (using the approximate values for Σ_x^{\max}) provided by Theorem 1 corresponds to $\bar{M} = 259$. The large magnitude of this value is due to some conservative steps in the proof technique (compare the steps between (42) and (45) in the proof of Theorem 1 in Appendix A), in which we bound the variable weighting matrix of the prior by the maximal possible weighting matrix. Note that in the simulation example, we choose the horizon length M to achieve a good performance in practice (as commonly done in the MHE literature), which was already the case for $M = 15$.

B. Comparison to further GP/model-based MHE schemes

In this section, we compare the performance of the GP-based MHE scheme (5) to different GP-based and model-based MHE schemes.

First, we consider another GP-based MHE scheme, in which we also approximate the system dynamics by the posterior means of GPs, but use constant matrices in the cost function (5e) instead of the varying matrices that account for the uncertainties in the learned model (abbreviated by "GP const."). Furthermore, we implement a model-based MHE scheme as suggested in [3] (called "MB const."). Finally, we consider another model-based MHE scheme similar to the one proposed in [3], but with an EKF update in the prior weighting, as detailed in [40] (called "MB EKF"). To compare the schemes, we use the same horizon length M , the same discount factor η , the same true initial condition, the same prior estimate, the same noise realizations, and (where applicable) the same weighting matrices. The performance of the different schemes is illustrated in Figure 1. It can be seen that the GP-based MHE scheme presented in this paper and

⁶The implementation of the GP-based MHE scheme is publicly available at: <https://doi.org/10.25835/yc7erc4p>

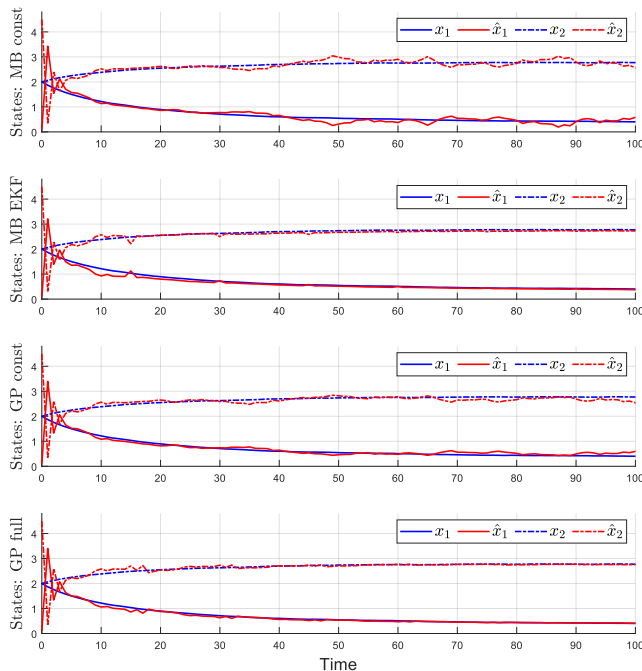


Fig. 1: Simulation examples of the implemented MHE schemes for system (37). In the first plot (top), the performance of a model-based MHE scheme as proposed in [3] is illustrated (called “MB const”). In the following plot (called “MB EKF”), we illustrate the performance of a model-based MHE scheme similar to [3], but with an EKF update in the prior weighting, as proposed in [40]. In the third plot, we show the performance of a GP-based MHE scheme similar to (5), but with constant P , Q , and R matrices (denoted by “GP const”). In the last plot, we illustrate the performance of the GP-based MHE scheme as introduced in (5) (denoted by “GP full”).

the model-based MHE scheme with an EKF update show the best performance.

To compare the different schemes in more detail, we consider 100 different initial conditions (sampled uniformly from the interval $x(0) \in [1, 3]^2$) and 100 different noise realizations (with the same means μ_w , μ_v and variances Σ_w , Σ_v as specified above) and simulate the four different MHE schemes as described above. Table I shows the mean squared error (MSE) (averaged over the 100 simulations), defined as $\text{MSE} := \frac{1}{nT} \sum_{i=1}^T \sum_{j=1}^n (x_j(i) - \hat{x}_j(i))^2$, where T denotes the number of time steps, here $T = 150$, and the mean absolute error (MAE) (also averaged over the 100 simulations), defined as $\text{MAE} := \frac{1}{nT} \sum_{i=1}^T \sum_{j=1}^n |x_j(i) - \hat{x}_j(i)|$. Furthermore, we report the average computation times (to compute one state estimate) in Table I. We obtained the simulations using a standard PC (Intel(R) Core(TM) i7-10875H CPU @ 2.30GHz (16 CPUs) processor with 16 GB RAM).

From Table I, we conclude that the GP-based MHE scheme as proposed in (5) is computationally demanding. This is not surprising, since we combine two computationally demanding techniques: Gaussian processes and MHE. When considering constant weighting matrices, the computation time decreases substantially, mainly because no inversion of the weighting matrices in the cost function is necessary anymore. Moreover, this method takes more time than the model-based MHE

schemes, since the computation of the posterior mean is much more demanding than the evaluation the true functions f and h .

In turn, the MAE and the MSE of the proposed MHE scheme (5) are (much) better compared to the MAE and the MSE of the GP-based MHE scheme considering constant weighting matrices. This observation underlines the importance to consider the uncertainty of the learned model in the weighting matrices. In particular, this shows how the uncertainty quantification which is inherent to GP regression can beneficially be incorporated into MHE in order to improve the estimation performance. The GP-based MHE scheme (5) even slightly outperforms the model-based MHE scheme proposed in [3], where perfect model knowledge was assumed. In the model-based MHE scheme proposed in [3] (as well as in many other model-based MHE schemes in the literature), constant weighting matrices are used. This results in a trade-off: one can trust the prior (P), the model (Q), or the measurements (R). In the example above, we typically have a bad prior available. To compensate this bad prior, we choose a small weight for P (and a rather large weight on R), such that the estimates converge quickly. However, in the steady state, this choice implies that we trust the noisy measurements a lot. Consequently, the state estimates fluctuate strongly as visible in plot referred to as “MB const” in Figure 1 (which explains the large MAE). To counteract this observation, one can design a model-based MHE scheme with a weighting on the prior that is updated according to the EKF update rule, compare [40] for details. In that case, we quantify the uncertainty of the prior estimate and use this uncertainty in the cost function. In that case, we have initially a low weight on the prior. As soon as the estimates improve, the weighting on the prior increases, which reduces the fluctuations in the state estimates, especially in the steady state. This model-based MHE scheme outperforms all other schemes due to the described choice of the weighting matrices and due to the perfect model knowledge.

In conclusion, note that the GP-based MHE scheme (5), for which no traditional system identification technique based on first principles, heuristics or expert knowledge has been applied, outperforms the model-based MHE scheme without EKF update (but perfect model knowledge) and performs only slightly worse than the model-based MHE scheme with an EKF update (again considering perfect model knowledge). These results suggest that the GP-based MHE can be an interesting alternative in applications with large sampling times (and hence computation times do not play a crucial role), such as, e.g., in process or biomedical engineering. In order to ensure real-time applicability also in systems with small sampling times, different extensions will be examined in future work (compare Section VII).

VII. CONCLUSION AND OUTLOOK

In this paper, we introduced a novel GP-based MHE scheme. The scheme advances state of the art MHE schemes by (i) approximating the system dynamics using the posterior means of GPs, and (ii) considering the uncertainty of the learned model directly in the cost function of the MHE

	MAE	MSE	$\bar{\tau}$ in s
Model-based MHE const. [3]	0.1273	0.0784	0.0234
Model-based MHE (with EKF update)	0.0522	0.0667	0.0216
GP-based MHE const.	0.3124	0.1628	0.4067
GP-based MHE (5)	0.0790	0.0690	4.1140

TABLE I: Performance comparison of four different MHE schemes. We consider (i) a model-based MHE scheme with perfect model knowledge [3] (ii) a model-based MHE scheme with perfect model knowledge similar to [3], but with an EKF update (compare [40]), (iii) a GP-based MHE scheme where we consider constant weighting matrices (but still approximate the dynamics by the posterior means), (vi) the GP-based MHE scheme as suggested in (5). The last column states the mean computation times to compute one state estimate.

scheme. We proved pRES of the GP-based MHE scheme based on standard assumptions. Moreover, we showed that nonlinear detectability (here δ -IOSS) can be preserved for the learned system if the true (unknown) system is δ -IOSS and the approximation error is small enough. We applied the GP-based scheme to a batch reactor example and showed that the proposed GP-based MHE scheme performs similarly well as model-based MHE schemes, where the model is exact.

The key idea of the proposed framework is to combine GPs and MHE, which are both computationally demanding. An interesting subject for future research is whether sparse GP techniques, such as e.g., sparse spectrum approximation [41] or sparse GPs using pseudo inputs [42] (also called fully independent training conditional model) and/or suboptimal MHE techniques [28] can result in a comparable performance while reducing the computational complexity. Furthermore, the proposed scheme is crucially based on offline available state measurements (often referred to as ground truth data in the machine learning literature [12], [14]) to train the GPs. If one was able to relax this assumption, the results of this work could be applied to a broader range of applications.

REFERENCES

- [1] J. B. Rawlings, D. Q. Mayne, and M. Diehl, *Model predictive control: theory, computation, and design*, 2nd ed. Nob Hill Publishing Madison, WI, 2020.
- [2] D. A. Allan and J. B. Rawlings, “Robust stability of full information estimation,” *SIAM Journal on Control and Optimization*, vol. 59, no. 5, pp. 3472–3497, 2021.
- [3] J. D. Schiller, S. Muntwiler, J. Köhler, M. N. Zeilinger, and M. A. Müller, “A Lyapunov function for robust stability of moving horizon estimation,” *IEEE Transactions on Automatic Control*, pp. 1–16, 2023.
- [4] A. Alessandri, M. Baglietto, G. Battistelli, and M. Gaggero, “Moving-horizon state estimation for nonlinear systems using neural networks,” *IEEE Transactions on Neural Networks*, vol. 22, no. 5, pp. 768–780, 2011.
- [5] W. Cao, J. Duan, S. E. Li, C. Chen, C. Liu, and Y. Wang, “Primal-dual estimator learning method with feasibility and near-optimality guarantees,” in *IEEE 61st Conference on Decision and Control (CDC)*. IEEE, 2022, pp. 4104–4111.
- [6] C. E. Rasmussen, C. K. Williams *et al.*, *Gaussian processes for machine learning*. Springer, 2006, vol. 1.
- [7] T. Beckers, D. Kulić, and S. Hirche, “Stable Gaussian process based tracking control of Euler–Lagrange systems,” *Automatica*, vol. 103, pp. 390–397, 2019.
- [8] M. Maiworm, D. Limon, and R. Findeisen, “Online learning-based model predictive control with Gaussian process models and stability guarantees,” *International Journal of Robust and Nonlinear Control*, vol. 31, no. 18, pp. 8785–8812, 2021.
- [9] L. Hewing, J. Kabzan, and M. N. Zeilinger, “Cautious model predictive control using Gaussian process regression,” *IEEE Transactions on Control Systems Technology*, vol. 28, no. 6, pp. 2736–2743, 2019.
- [10] M. Buisson-Fenet, V. Morgenthaler, S. Trimpe, and F. Di Meglio, “Joint state and dynamics estimation with high-gain observers and Gaussian process models,” in *2021 American Control Conference (ACC)*. IEEE, 2021, pp. 4027–4032.
- [11] A. Capone and S. Hirche, “Interval observers for a class of nonlinear systems using Gaussian process models,” in *2019 18th European Control Conference (ECC)*. IEEE, 2019, pp. 1350–1355.
- [12] J. Ko and D. Fox, “GP-BayesFilters: Bayesian filtering using Gaussian process prediction and observation models,” *Autonomous Robots*, vol. 27, pp. 75–90, 2009.
- [13] J. Ko, D. J. Klein, D. Fox, and D. Haehnel, “GP-UKF: Unscented Kalman filters with Gaussian process prediction and observation models,” in *2007 IEEE/RSJ International Conference on Intelligent Robots and Systems*. IEEE, 2007, pp. 1901–1907.
- [14] M. P. Deisenroth, M. F. Huber, and U. D. Hanebeck, “Analytic moment-based Gaussian process filtering,” in *Proceedings of the 26th annual international conference on machine learning*, 2009, pp. 225–232.
- [15] M. P. Deisenroth, *Efficient reinforcement learning using Gaussian processes*. KIT Scientific Publishing, 2010, vol. 9.
- [16] C. H. Tong, P. Furgale, and T. D. Barfoot, “Gaussian process Gauss-Newton for non-parametric simultaneous localization and mapping,” *The International Journal of Robotics Research*, vol. 32, no. 5, pp. 507–525, 2013.
- [17] C. H. Tong and T. D. Barfoot, “Gaussian process Gauss-Newton for 3D laser-based visual odometry,” in *2013 IEEE International Conference on Robotics and Automation*. IEEE, 2013, pp. 5204–5211.
- [18] W. Choo and E. Kayacan, “Data-based MHE for agile quadrotor flight,” in *2023 IEEE/RSJ International Conference on Intelligent Robots and Systems (IROS)*, 2023, pp. 4307–4314.
- [19] T. M. Wolff, V. G. Lopez, and M. A. Müller, “Robust stability of Gaussian process based moving horizon estimation,” in *2023 62nd IEEE Conference on Decision and Control (CDC)*, 2023, pp. 4087–4093.
- [20] A. Lederer, J. Umlauf, and S. Hirche, “Uniform error bounds for Gaussian process regression with application to safe control,” *Advances in Neural Information Processing Systems*, vol. 32, 2019.
- [21] M. S. Turan and G. Ferrari-Trecate, “Data-driven unknown-input observers and state estimation,” *IEEE Control Systems Letters*, vol. 6, pp. 1424–1429, 2022.
- [22] T. M. Wolff, V. G. Lopez, and M. A. Müller, “Robust data-driven moving horizon estimation for linear discrete-time systems,” *arXiv preprint arXiv:2210.09017*, 2022.
- [23] T. Gräber, S. Lupberger, M. Unterreiner, and D. Schramm, “A hybrid approach to side-slip angle estimation with recurrent neural networks and kinematic vehicle models,” *IEEE Transactions on Intelligent Vehicles*, vol. 4, no. 1, pp. 39–47, 2019.
- [24] S. F. G. Ehlers, Z. Ziaukas, J.-P. Kobler, and H.-G. Jacob, “State and parameter estimation in a semitrailer for different loading conditions only based on trailer signals,” in *2022 American Control Conference (ACC)*, 2022, pp. 2353–2360.
- [25] J. Ko and D. Fox, “Learning GP-BayesFilters via Gaussian process latent variable models,” *Autonomous Robots*, vol. 30, pp. 3–23, 2011.
- [26] A. McHutchon and C. Rasmussen, “Gaussian process training with input noise,” *Advances in neural information processing systems*, vol. 24, 2011.
- [27] S. Knüfer and M. A. Müller, “Robust global exponential stability for moving horizon estimation,” in *2018 IEEE Conference on Decision and Control (CDC)*, 2018, pp. 3477–3482.
- [28] J. D. Schiller and M. A. Müller, “Suboptimal nonlinear moving horizon estimation,” *IEEE Transactions on Automatic Control*, vol. 68, no. 4, pp. 2199–2214, 2022.
- [29] S. Knüfer and M. A. Müller, “Nonlinear full information and moving horizon estimation: Robust global asymptotic stability,” *Automatica*, vol. 150, p. 110603, 2023.
- [30] H. Arezki, A. Alessandri, and A. Zemouche, “Robust convergence analysis of moving-horizon estimator for LPV discrete-time systems,” *IFAC-PapersOnLine*, vol. 56, no. 2, pp. 11 578–11 583, 2023, 22nd IFAC World Congress.
- [31] M. P. Deisenroth, D. Fox, and C. E. Rasmussen, “Gaussian processes for data-efficient learning in robotics and control,” *IEEE transactions on pattern analysis and machine intelligence*, vol. 37, no. 2, pp. 408–423, 2013.
- [32] D. A. Allan, J. Rawlings, and A. R. Teel, “Nonlinear detectability and incremental input/output-to-state stability,” *SIAM Journal on Control and Optimization*, vol. 59, no. 4, pp. 3017–3039, 2021.

- [33] N. Srinivas, A. Krause, S. M. Kakade, and M. W. Seeger, "Information-theoretic regret bounds for Gaussian process optimization in the bandit setting," *IEEE Transactions on Information Theory*, vol. 58, no. 5, pp. 3250–3265, 2012.
- [34] S. R. Chowdhury and A. Gopalan, "On kernelized multi-armed bandits," in *Proceedings of the 34th International Conference on Machine Learning*, ser. Proceedings of Machine Learning Research, D. Precup and Y. W. Teh, Eds., vol. 70. PMLR, 2017, pp. 844–853.
- [35] C. Fiedler, C. W. Scherer, and S. Trimpe, "Practical and rigorous uncertainty bounds for Gaussian process regression," in *Proceedings of the AAAI conference on artificial intelligence*, vol. 35, no. 8, 2021, pp. 7439–7447.
- [36] A. Christmann and I. Steinwart, "Support vector machines," 2008.
- [37] T. Beckers, "Gaussian process based modeling and control with guarantees," Ph.D. dissertation, Technische Universität München, 2020.
- [38] J. A. Andersson, J. Gillis, G. Horn, J. B. Rawlings, and M. Diehl, "CasADi: a software framework for nonlinear optimization and optimal control," *Mathematical Programming Computation*, vol. 11, pp. 1–36, 2019.
- [39] A. Wächter and L. T. Biegler, "On the implementation of an interior-point filter line-search algorithm for large-scale nonlinear programming," *Mathematical Programming*, vol. 106, pp. 25–57, 2006.
- [40] M. J. Tenny and J. B. Rawlings, "Efficient moving horizon estimation and nonlinear model predictive control," in *Proceedings of the 2002 American Control Conference*, vol. 6. IEEE, 2002, pp. 4475–4480.
- [41] M. Lázaro-Gredilla, J. Quinero-Candela, C. E. Rasmussen, and A. R. Figueiras-Vidal, "Sparse spectrum Gaussian process regression," *The Journal of Machine Learning Research*, vol. 11, pp. 1865–1881, 2010.
- [42] E. Snelson and Z. Ghahramani, "Sparse Gaussian processes using pseudo-inputs," *Advances in Neural Information Processing Systems*, vol. 18, 2005.



Tobias M. Wolff received a M.Sc. degree in Electrical Engineering from the Karlsruhe Institute of Technology and from the Grenoble Institute of Technology, both in 2021. He is currently a PhD student at the Institute of Automatic Control, Leibniz University Hannover, Germany. His main research interests are data- and learning-based estimation and biomedical applications.



Victor G. Lopez received his B.Sc. degree in Communications and Electronics Engineering from the Universidad Autonoma de Campeche, in Campeche, Mexico, in 2010, the M.Sc. degree in Electrical Engineering from the Research and Advanced Studies Center (Cinvestav), in Guadalajara, Mexico, in 2013, and his Ph.D. degree in Electrical Engineering from the University of Texas at Arlington, Texas, USA, in 2019. In 2015 Victor was a Lecturer at the Western Technological Institute of Superior Studies (ITESO)

in Guadalajara, Mexico. From August 2019 to June 2020, he was a postdoctoral researcher at the University of Texas at Arlington Research Institute and an Adjunct Professor in the Electrical Engineering department at UTA. Victor is currently a postdoctoral researcher at the Institute of Automatic Control, Leibniz University Hannover, Germany. His research interest include cyber-physical systems, reinforcement learning, game theory, distributed control and robust control.



Matthias A. Müller (Senior Member, IEEE) received a Diploma degree in engineering cybernetics from the University of Stuttgart, Germany, an M. Sc. in electrical and computer engineering from the University of Illinois at Urbana-Champaign, US (both in 2009), and a Ph. D. from the University of Stuttgart in 2014. Since 2019, he is Director of the Institute of Automatic Control and Full Professor at the Leibniz University Hannover, Germany. His research interests include nonlinear control and estimation, model predictive control, and data- and learning-based control, with application in different fields including biomedical engineering and robotics. He has received various awards for his work, including the 2015 European Systems & Control PhD Thesis Award, the inaugural Brockett-Willems Outstanding Paper Award for the best paper published in Systems & Control Letters in the period 2014-2018, an ERC starting grant in 2020, the IEEE CSS George S. Axelby Outstanding Paper Award 2022, and the Journal of Process Control Paper Award 2023. He serves as an associate editor for Automatica, as editor of the International Journal of Robust and Nonlinear Control and as a member of the Conference Editorial Board of the IEEE Control Systems Society.

APPENDIX

A. Proof of Theorem 1

The proof of Theorem 1 is based on the developments shown in [3]. However, here we consider an MHE scheme based on learned dynamics (and not based on perfect model knowledge). Additionally, we consider a cost function with varying weights, which also requires some adaptations in the proof. Here, we mainly comment on the steps that are conceptually different from the proof in [3], without describing the similar steps of the proof in all detail.

Proof: The constraints in the MHE problem guarantee that the optimal estimated system trajectory (denoted by $\hat{x}(j|t)$, $u(j)$, $\hat{w}(j|t)$, $\hat{v}(j|t)$ for all $j \in \mathbb{I}_{[t-M_t, t-1]}$) satisfies the learned system dynamics (2). In general, the unknown (true) system trajectory cannot necessarily be represented by the learned dynamics due to approximation errors. To represent the true system trajectory using the learned dynamics, we use the introduced auxiliary variables in \check{w} (3) and in \check{v} (4). We exploit that, due to (5c), $m_{+,y}(d(j)|D^{dt}, Y^{dt}) - m_{+,y}(\hat{d}(j|t)|D^{dt}, Y^{dt}) = \hat{v}(j|t) - \check{v}(j)$ for all $j \in \mathbb{I}_{[t-M_t, t-1]}$. Furthermore, we apply inequality (17b) M_t times along (i) the real and (ii) the optimal estimated trajectories, which yields

$$\begin{aligned}
 & W_\delta(\hat{x}(t), x(t)) \\
 & \stackrel{(17b)}{\leq} \sum_{j=1}^{M_t} \eta^{j-1} \left(\|\hat{w}(t-j|t) - \check{w}(t-j)\|_{(\Sigma_x^{\max})^{-1}}^2 \right. \\
 & \quad \left. + \|\hat{v}(t-j|t) - \check{v}(t-j)\|_{(\Sigma_y^{\max})^{-1}}^2 \right) \\
 & \quad + \eta^{M_t} W_\delta(\hat{x}(t-M_t|t), x(t-M_t)).
 \end{aligned}$$

Moreover, using (17a), the triangle inequality, the Cauchy-

Schwarz inequality, and Young's inequality, it holds

$$\begin{aligned}
W_\delta(\hat{x}(t), x(t)) &\leq \sum_{j=1}^{M_t} \eta^{j-1} \left(2\|\hat{w}(t-j|t)\|_{(\Sigma_x^{\max})^{-1}}^2 + 2\|\check{w}(t-j)\|_{(\Sigma_x^{\max})^{-1}}^2 \right. \\
&\quad \left. + 2\|\hat{v}(t-j|t)\|_{(\Sigma_y^{\max})^{-1}}^2 + 2\|\check{v}(t-j)\|_{(\Sigma_y^{\max})^{-1}}^2 \right) \\
&\quad + 2\eta^{M_t} \|\hat{x}(t-M_t) - x(t-M_t)\|_{(\Sigma_x^{\max})^{-1}}^2 \\
&\quad + 2\eta^{M_t} \|\hat{x}(t-M_t|t) - \hat{x}(t-M_t)\|_{(\Sigma_x^{\max})^{-1}}^2.
\end{aligned}$$

By rearranging the terms, we obtain

$$\begin{aligned}
W_\delta(\hat{x}(t), x(t)) &\leq 2\eta^{M_t} \|\hat{x}(t-M_t) - x(t-M_t)\|_{(\Sigma_x^{\max})^{-1}}^2 \\
&\quad + \sum_{j=1}^{M_t} 2\eta^{j-1} \left(\|\check{w}(t-j)\|_{(\Sigma_x^{\max})^{-1}}^2 + \|\check{v}(t-j)\|_{(\Sigma_y^{\max})^{-1}}^2 \right) \\
&\quad + 2\eta^{M_t} \|\hat{x}(t-M_t|t) - \hat{x}(t-M_t)\|_{(\Sigma_x^{\max})^{-1}}^2 \\
&\quad + \sum_{j=1}^{M_t} 2\eta^{j-1} \left(\|\hat{w}(t-j|t)\|_{(\Sigma_x^{\max})^{-1}}^2 \right. \\
&\quad \quad \left. + \|\hat{v}(t-j|t)\|_{(\Sigma_y^{\max})^{-1}}^2 \right) \\
&=: 2\eta^{M_t} \|\hat{x}(t-M_t) - x(t-M_t)\|_{(\Sigma_x^{\max})^{-1}}^2 \\
&\quad + \sum_{j=1}^{M_t} 2\eta^{j-1} \left(\|\check{w}(t-j)\|_{(\Sigma_x^{\max})^{-1}}^2 + \|\check{v}(t-j)\|_{(\Sigma_y^{\max})^{-1}}^2 \right) \\
&\quad + J_{\min}(\hat{x}(t-M_t|t), \hat{w}(\cdot|t), \hat{v}(\cdot|t), t). \tag{38}
\end{aligned}$$

Note that $J_{\min}(\hat{x}(t-M_t|t), \hat{w}(\cdot|t), \hat{v}(\cdot|t), t)$ does not correspond to the optimal cost of problem (5). In fact, $J_{\min}(\hat{x}(t-M_t|t), \hat{w}(\cdot|t), \hat{v}(\cdot|t), t)$ corresponds to the cost of the optimal trajectory, when $(\Sigma_x^{\max})^{-1}$, $(\Sigma_y^{\max})^{-1}$ are considered in the cost function (5e) (but *not* the variable matrices $(\Sigma_{x, \hat{d}(t-M_t-1|t-M_t)})^{-1}$, $(\Sigma_{x, \bar{d}(t-j|t)})^{-1}$, and $(\Sigma_{y, \bar{d}(t-j|t)})^{-1}$). Next, we upper bound $J_{\min}(\hat{x}(t-M_t|t), \hat{w}(\cdot|t), \hat{v}(\cdot|t), t)$ as follows

$$\begin{aligned}
J_{\min}(\hat{x}(t-M_t|t), \hat{w}(\cdot|t), \hat{v}(\cdot|t), t) &\leq J(\hat{x}(t-M_t|t), \hat{w}(\cdot|t), \hat{v}(\cdot|t), t) \tag{39} \\
&\leq J(x(t-M_t), \check{w}(\cdot), \check{v}(\cdot), t)
\end{aligned}$$

where we recall that $J(\hat{x}(t-M_t|t), \hat{w}(\cdot|t), \hat{v}(\cdot|t), t) = J^*$ is the optimal value function of problem (5). The first inequality holds by (15) and (16), and the second is due to optimality (i.e., the true unknown system trajectory $x(\cdot), \check{w}(\cdot), \check{v}(\cdot)$ is a feasible but in general suboptimal solution to problem (5)).

We consider these bounds in inequality (38) and obtain

$$\begin{aligned}
W_\delta(\hat{x}(t), x(t)) &\leq 2\eta^{M_t} \|\hat{x}(t-M_t) - x(t-M_t)\|_{(\Sigma_x^{\max})^{-1}}^2 \\
&\quad + \sum_{j=1}^{M_t} 2\eta^{j-1} \left(\|\check{w}(t-j)\|_{(\Sigma_x^{\max})^{-1}}^2 + \|\check{v}(t-j)\|_{(\Sigma_y^{\max})^{-1}}^2 \right) \\
&\quad + 2\eta^{M_t} \|\hat{x}(t-M_t) - x(t-M_t)\|_{(\Sigma_{x, \hat{d}(t-M_t-1|t-M_t)})^{-1}}^2 \\
&\quad + \sum_{j=1}^{M_t} 2\eta^{j-1} \left(\|\check{w}(t-j)\|_{(\Sigma_{x, d(t-j)})^{-1}}^2 \right. \\
&\quad \quad \left. + \|\check{v}(t-j)\|_{(\Sigma_{y, d(t-j)})^{-1}}^2 \right), \tag{40}
\end{aligned}$$

where $\Sigma_{x, d(t-j)}$ and $\Sigma_{y, d(t-j)}$ denote the uncertainty provided by the GPs when the true system trajectory is considered in the weighting matrices (6) - (7), initialized with $\Sigma_{x, d(t-M_t-1)} = 0$ (compare Footnote 1). Using (15) and (16), we obtain

$$\begin{aligned}
W_\delta(\hat{x}(t), x(t)) &\leq 4\eta^{M_t} \|\hat{x}(t-M_t) - x(t-M_t)\|_{(\Sigma_{x, \hat{d}(t-M_t-1|t-M_t)})^{-1}}^2 \\
&\quad + \sum_{j=1}^{M_t} 4\eta^{j-1} \left(\|\check{w}(t-j)\|_{(\Sigma_{x, d(t-j)})^{-1}}^2 \right. \\
&\quad \quad \left. + \|\check{v}(t-j)\|_{(\Sigma_{y, d(t-j)})^{-1}}^2 \right) \tag{41} \\
&\leq 4\lambda_{\max} \left((\Sigma_x^{\min})^{-1}, (\Sigma_x^{\max} + \varepsilon I)^{-1} \right) \eta^{M_t} \\
&\quad \times W_\delta(\hat{x}(t-M_t), x(t-M_t)) \\
&\quad + \sum_{j=1}^{M_t} 4\eta^{j-1} \left(\|\check{w}(t-j)\|_{(\Sigma_{x, d(t-j)})^{-1}}^2 \right. \\
&\quad \quad \left. + \|\check{v}(t-j)\|_{(\Sigma_{y, d(t-j)})^{-1}}^2 \right).
\end{aligned}$$

We choose M large enough such that

$$\mu^M := 4\lambda_{\max} \left((\Sigma_x^{\min})^{-1}, (\Sigma_x^{\max} + \varepsilon I)^{-1} \right) \eta^M < 1 \tag{42}$$

with $\mu \in [0, 1)$, and obtain for all $t \in \mathbb{I}_{\geq M}$

$$\begin{aligned}
W_\delta(\hat{x}(t), x(t)) &\leq \mu^M W_\delta(\hat{x}(t-M), x(t-M)) \\
&\quad + \sum_{j=1}^M 4\eta^{j-1} \left(\|\check{w}(t-j)\|_{(\Sigma_{x, d(t-j)})^{-1}}^2 \right. \\
&\quad \quad \left. + \|\check{v}(t-j)\|_{(\Sigma_{y, d(t-j)})^{-1}}^2 \right). \tag{43}
\end{aligned}$$

Performing similar steps as the ones in the proof of [3, Cor. 1] results in the following state estimation error bound which we show in the following for completeness. We consider some time instant $t = \kappa M + l$ with $l \in \mathbb{I}_{[0, M-1]}$ and $\kappa \in \mathbb{I}_{\geq 0}$. Using (42), we obtain

$$\begin{aligned}
W_\delta(\hat{x}(l), x(l)) &\leq 4\eta^l \|\hat{x}(0) - x(0)\|_{(\Sigma_{x, \hat{d}(-1|0)})^{-1}}^2 \\
&\quad + 4 \sum_{j=1}^l \eta^{j-1} \left(\|\check{w}(l-j)\|_{(\Sigma_{x, d(l-j)})^{-1}}^2 \right. \\
&\quad \quad \left. + \|\check{v}(l-j)\|_{(\Sigma_{y, d(l-j)})^{-1}}^2 \right). \tag{44}
\end{aligned}$$

The bound (45) will be used below. We can now apply (44) κ times. This means that we recursively iterate a contraction.

Within each interval, we set the initial uncertainty to zero, compare the explanations in Subsection III-B (paragraph below (13)) and Footnote 1 in Section IV. With a slight abuse of notation, we do not specify this initialization in the following to improve the readability of the proof. We obtain

$$\begin{aligned}
& W_\delta(\hat{x}(t), x(t)) \\
& \leq \mu^{\kappa M} W_\delta(\hat{x}(l) - x(l)) \\
& + 4 \sum_{i=0}^{\kappa-1} \mu^{iM} \sum_{j=1}^M \eta^{j-1} \left(\|\check{w}(t - iM - j)\|_{(\Sigma_{x,d(t-iM-j)})^{-1}}^2 \right. \\
& \quad \left. + \|\check{v}(t - iM - j)\|_{(\Sigma_{y,d(t-iM-j)})^{-1}}^2 \right) \\
& \stackrel{(45)}{\leq} \mu^{\kappa M} \left(4\eta^l \|\hat{x}(0) - x(0)\|_{(\Sigma_{x,\hat{d}(-1|0)})^{-1}}^2 \right. \\
& + 4 \sum_{j=1}^l \eta^{j-1} \left(\|\check{w}(l - j)\|_{(\Sigma_{x,d(l-j)})^{-1}}^2 \right. \\
& \quad \left. + \|\check{v}(l - j)\|_{(\Sigma_{y,d(l-j)})^{-1}}^2 \right) \\
& + 4 \sum_{i=0}^{\kappa-1} \mu^{iM} \sum_{j=1}^M \eta^{j-1} \left(\|\check{w}(t - iM - j)\|_{(\Sigma_{x,d(t-iM-j)})^{-1}}^2 \right. \\
& \quad \left. + \|\check{v}(t - iM - j)\|_{(\Sigma_{y,d(t-iM-j)})^{-1}}^2 \right)
\end{aligned}$$

Using $\eta \leq \mu$, we have

$$\begin{aligned}
& W_\delta(\hat{x}(t), x(t)) \\
& \leq 4\mu^t \|\hat{x}(0) - x(0)\|_{(\Sigma_{x,\hat{d}(-1|0)})^{-1}}^2 \\
& + 4 \sum_{j=1}^l \mu^{\kappa M + j - 1} \left(\|\check{w}(l - j)\|_{(\Sigma_{x,d(l-j)})^{-1}}^2 \right. \\
& \quad \left. + \|\check{v}(l - j)\|_{(\Sigma_{y,d(l-j)})^{-1}}^2 \right) \\
& + 4 \sum_{i=0}^{\kappa-1} \sum_{j=1}^M \mu^{iM + j - 1} \left(\|\check{w}(t - iM - j)\|_{(\Sigma_{x,d(t-iM-j)})^{-1}}^2 \right. \\
& \quad \left. + \|\check{v}(t - iM - j)\|_{(\Sigma_{y,d(t-iM-j)})^{-1}}^2 \right) \\
& = 4\mu^t \|\hat{x}(0) - x(0)\|_{(\Sigma_{x,\hat{d}(-1|0)})^{-1}}^2 \\
& + 4 \sum_{q=0}^{t-1} \mu^q \left(\|\check{w}(t - q - 1)\|_{(\Sigma_{x,d(t-q-1)})^{-1}}^2 \right. \\
& \quad \left. + \|\check{v}(t - q - 1)\|_{(\Sigma_{y,d(t-q-1)})^{-1}}^2 \right).
\end{aligned}$$

From here on, consider

$$\begin{aligned}
& \|\hat{x}(t) - x(t)\|_{(\Sigma_x^{\max} + \varepsilon I)^{-1}} \\
& \stackrel{(17a)}{\leq} \sqrt{W_\delta(\hat{x}(t), x(t))} \\
& \leq 2\sqrt{\mu^t} \|\hat{x}(0) - x(0)\|_{(\Sigma_{x,\hat{d}(-1|0)})^{-1}} \\
& + 2 \sum_{q=0}^{t-1} \sqrt{\mu^q} \left(\|\check{w}(t - q - 1)\|_{(\Sigma_{x,d(t-q-1)})^{-1}} \right. \\
& \quad \left. + \|\check{v}(t - q - 1)\|_{(\Sigma_{y,d(t-q-1)})^{-1}} \right), \tag{46}
\end{aligned}$$

where we exploited that $\sqrt{a+b} \leq \sqrt{a} + \sqrt{b}$ for any $a, b \geq 0$. Finally, we consider

$$\begin{aligned}
& \sum_{q=0}^{t-1} \sqrt{\mu^q} \|\check{w}(t - q - 1)\|_{(\Sigma_{x,d(t-q-1)})^{-1}} \\
& \leq \sum_{q=0}^{t-1} \sqrt[4]{\mu^q} \max_{q \in \mathbb{I}_{[0,t-1]}} \left\{ \sqrt[4]{\mu^q} \|\check{w}(t - q - 1)\|_{(\Sigma_{x,d(t-q-1)})^{-1}} \right\} \\
& \leq \frac{1}{1 - \sqrt[4]{\mu}} \max_{q \in \mathbb{I}_{[0,t-1]}} \left\{ \sqrt[4]{\mu^q} \|\check{w}(t - q - 1)\|_{(\Sigma_{x,d(t-q-1)})^{-1}} \right\}
\end{aligned}$$

to obtain the max-based formulation from (14) in Definition 1. Inserting the bound into (46) and proceeding analogously for \check{v} results in

$$\begin{aligned}
& \|\hat{x}(t) - x(t)\|_{(\Sigma_x^{\max} + \varepsilon I)^{-1}} \\
& \leq 2\sqrt{\mu^t} \|\hat{x}(0) - x(0)\|_{(\Sigma_{x,\hat{d}(-1|0)})^{-1}} \\
& + \max_{q \in \mathbb{I}_{[0,t-1]}} \left\{ \frac{2}{1 - \sqrt[4]{\mu}} \sqrt[4]{\mu^q} \|\check{w}(t - q - 1)\|_{(\Sigma_{x,d(t-q-1)})^{-1}} \right\} \\
& + \max_{q \in \mathbb{I}_{[0,t-1]}} \left\{ \frac{2}{1 - \sqrt[4]{\mu}} \sqrt[4]{\mu^q} \|\check{v}(t - q - 1)\|_{(\Sigma_{y,d(t-q-1)})^{-1}} \right\}.
\end{aligned}$$

Using

$$\begin{aligned}
& a + \max_i \{b_i\} + \max_i \{c_i\} \\
& \leq \max\{3a, \max_i \{3b_i\}, \max_i \{3c_i\}\} \tag{47}
\end{aligned}$$

for any $a, b_i, c_i \geq 0$ for $i = 1, \dots, t-1$, we obtain

$$\begin{aligned}
& \|\hat{x}(t) - x(t)\|_{(\Sigma_x^{\max} + \varepsilon I)^{-1}} \\
& \leq \max \left\{ 6\sqrt{\mu^t} \|\hat{x}(0) - x(0)\|_{(\Sigma_{x,\hat{d}(-1|0)})^{-1}}, \right. \\
& \quad \max_{q \in \mathbb{I}_{[0,t-1]}} \left\{ \frac{6}{1 - \sqrt[4]{\mu}} \sqrt[4]{\mu^q} \|\check{w}(t - q - 1)\|_{(\Sigma_{x,d(t-q-1)})^{-1}} \right\}, \\
& \quad \left. \max_{q \in \mathbb{I}_{[0,t-1]}} \left\{ \frac{6}{1 - \sqrt[4]{\mu}} \sqrt[4]{\mu^q} \|\check{v}(t - q - 1)\|_{(\Sigma_{y,d(t-q-1)})^{-1}} \right\} \right\}. \tag{48}
\end{aligned}$$

We replace \check{w} and \check{v} according to (3) and (4), respectively. Then, we apply the triangle inequality and bound the difference between the functions f, h and the posterior means $m_{+,x}, m_{+,y}$ by (18) and (19), respectively, which results in

$$\begin{aligned}
& \|\hat{x}(t) - x(t)\|_{(\Sigma_x^{\max} + \varepsilon I)^{-1}} \\
& \leq \max \left\{ 6\sqrt{\mu^t} \|\hat{x}(0) - x(0)\|_{(\Sigma_{x,\hat{d}(-1|0)})^{-1}}, \right. \\
& \quad \max_{q \in \mathbb{I}_{[0,t-1]}} \left\{ \frac{6\sqrt[4]{\mu^q}}{1 - \sqrt[4]{\mu}} (\|w(t - q - 1)\|_{(\Sigma_{x,d(t-q-1)})^{-1}} + \alpha_1^{\max}) \right\}, \\
& \quad \left. \max_{q \in \mathbb{I}_{[0,t-1]}} \left\{ \frac{6\sqrt[4]{\mu^q}}{1 - \sqrt[4]{\mu}} (\|v(t - q - 1)\|_{(\Sigma_{y,d(t-q-1)})^{-1}} \right. \right. \\
& \quad \left. \left. + \alpha_2^{\max}) \right\} \right\}. \tag{49}
\end{aligned}$$

Using that $\max_{q \in \mathbb{I}_{[0,t-1]}} \sqrt[4]{\mu^q} = 1$ and $a + b \leq \max\{2a, 2b\}$

for any $a, b \geq 0$, we have

$$\begin{aligned} & \|\hat{x}(t) - x(t)\|_{(\Sigma_x^{\max} + \varepsilon I)^{-1}} \\ & \leq \max \left\{ 6\sqrt{\mu}^t \|\hat{x}(0) - x(0)\|_{(\Sigma_x, \hat{d}(-1|0))^{-1}}, \right. \\ & \quad \max_{q \in \mathbb{I}_{[0, t-1]}} \left\{ \frac{12}{1 - \sqrt[4]{\mu}} \sqrt[4]{\mu}^q \|w(t-q-1)\|_{(\Sigma_x, d(t-q-1))^{-1}} \right\}, \\ & \quad \max_{q \in \mathbb{I}_{[0, t-1]}} \left\{ \frac{12}{1 - \sqrt[4]{\mu}} \sqrt[4]{\mu}^q \|v(t-q-1)\|_{(\Sigma_y, d(t-q-1))^{-1}} \right\}, \\ & \quad \left. \frac{12}{1 - \sqrt[4]{\mu}} \alpha_1^{\max}, \frac{12}{1 - \sqrt[4]{\mu}} \alpha_2^{\max} \right\}. \end{aligned} \quad (50)$$

Finally, we use α_{\max} to bound the last two terms of (50), which leads to the expression (20) of Theorem 1. ■

B. Proof of Corollary 1

Based on the adapted MHE scheme, one can obtain a similar result to Theorem 1, simply with $(\Sigma_x^{\max} + \varepsilon I)^{-1}$, $(\Sigma_x, \hat{d}(-1|0))^{-1}$, $(\Sigma_x, d(t-q-1))^{-1}$, $(\Sigma_y, d(t-q-1))^{-1}$, α_{\max} replaced by $(\tilde{\Sigma}_x^{\max} + \varepsilon I)^{-1}$, $(\tilde{\Sigma}_x, \hat{d}(-1|0))^{-1}$, $(\tilde{\Sigma}_x, d(t-q-1))^{-1}$, $(\tilde{\Sigma}_y, d(t-q-1))^{-1}$, $\tilde{\alpha}_{\max}$, respectively, where $\tilde{\alpha}_{\max}$ is defined analogously to α_{\max} . We can bound $\tilde{\alpha}_1^{\max}$ and $\tilde{\alpha}_2^{\max}$ (which are defined once again analogously to α_1^{\max} and α_2^{\max} in (18) and (19)) as follows

$$\tilde{\alpha}_1^{\max} \leq \sqrt{\lambda_{\max}((\tilde{\Sigma}_x^{\min})^{-1})} \times \sum_{i=1}^n \max_{x \in \mathbb{X}, u \in \mathbb{U}} \{ \|f_i(x, u) - m_{+,x_i}(d|D^{dt}, X_i^{dt})\| \}, \quad (51)$$

$$\tilde{\alpha}_2^{\max} \leq \sqrt{\lambda_{\max}((\tilde{\Sigma}_y^{\min})^{-1})} \times \sum_{i=1}^p \max_{x \in \mathbb{X}, u \in \mathbb{U}} \{ \|h_i(x, u) - m_{+,y_i}(d|D^{dt}, Y_i^{dt})\| \}. \quad (52)$$

From here on, we apply [35, Prop. 2] to probabilistically bound the difference between the true function components of f , h and the corresponding posterior means. For the components⁷ of f and h , this results in

$$\begin{aligned} & P\left(\|f_i(x, u) - m_{x_i}(d|D^{dt}, X_i^{dt})\| \right. \\ & \quad \leq B_{x_i} \sigma_{+,x_i}(d|D^d, X_i^d) + \eta_{N,x_i}(d), \forall x \in \mathbb{X}, u \in \mathbb{U} \Big) \\ & \quad \geq 1 - \delta \quad i = 1, \dots, n \end{aligned}$$

$$\begin{aligned} & P\left(\|h_j(x, u) - m_{y_j}(d|D^{dt}, Y_j^{dt})\| \right. \\ & \quad \leq B_{y_j} \sigma_{+,y_j}(d|D^d, Y_j^d) + \eta_{N,y_j}(d), \forall x \in \mathbb{X}, u \in \mathbb{U} \Big) \\ & \quad \geq 1 - \delta \quad j = 1, \dots, p. \end{aligned}$$

The probability that all the components of f jointly fulfill their bounds is lower bounded by $1 - n\delta$ (the same holds for h with probability $1 - p\delta$) by applying the union bound. We replace

⁷We assume for simplicity that the same value of δ has been chosen for all components of the functions f and h .

the right hand sides of (51) and (52) by these probabilistic bounds, i.e.,

$$P(\tilde{\alpha}_1^{\max} \leq \Delta_x^{\max}) \geq 1 - n\delta \quad (53)$$

$$P(\tilde{\alpha}_2^{\max} \leq \Delta_y^{\max}) \geq 1 - p\delta. \quad (54)$$

Finally, the probability that both $\alpha_1^{\max} \leq \Delta_x^{\max}$ and $\alpha_2^{\max} \leq \Delta_y^{\max}$ hold jointly is lower bounded by $1 - (n+p)\delta$. Using this bound in (50), we obtain the left-hand side of (31). ■

C. Proof of Theorem 2

Due to Assumption 3, the true system (1) admits a δ -IOSS Lyapunov function. We consider this δ -IOSS Lyapunov function, but replace the state transition function f by its approximation $m_{+,x}(x, u)$ from (2)

$$\begin{aligned} & W_\delta(m_{+,x}((x, u)|D^{dt}, X^{dt}) + w, \\ & \quad m_{+,x}((\tilde{x}, u)|D^{dt}, X^{dt}) + \tilde{w}) \\ & = W_\delta(m_{+,x}((x, u)|D^{dt}, X^{dt}) + w + f(x, u) - f(x, u), \\ & \quad m_{+,x}((\tilde{x}, u)|D^{dt}, X^{dt}) + \tilde{w} + f(\tilde{x}, u) - f(\tilde{x}, u)) \\ & = W_\delta(f(x, u) + w + m_{+,x}((x, u)|D^{dt}, X^{dt}) - f(x, u), \\ & \quad f(\tilde{x}, u) + \tilde{w} + m_{+,x}((\tilde{x}, u)|D^{dt}, X^{dt}) - f(\tilde{x}, u)), \end{aligned}$$

where we added zero in the first equality and then rearranged the terms. Now, we want to apply the dissipation inequality (32b), which holds for the original system. To this end, we introduce

$$w_{1d} := w + m_{+,x}((x, u)|D^{dt}, X^{dt}) - f(x, u) \quad (55)$$

$$\tilde{w}_{1d} := \tilde{w} + m_{+,x}((\tilde{x}, u)|D^{dt}, X^{dt}) - f(\tilde{x}, u). \quad (56)$$

with $w_{1d}, \tilde{w}_{1d} \in \mathbb{W}$ by Assumption 5 and $w, \tilde{w} \in \mathbb{W} \oplus \mathbb{E}_x$. Applying inequality (32b) results in

$$\begin{aligned} & W_\delta(m_{+,x}((x, u)|D^{dt}, X^{dt}) + w, \\ & \quad m_{+,x}((\tilde{x}, u)|D^{dt}, X^{dt}) + \tilde{w}) \\ & \leq \eta W_\delta(x, \tilde{x}) + \sigma_w(\|w_{1d} - \tilde{w}_{1d}\|) \\ & \quad + \sigma_h(\|h(x, u) - h(\tilde{x}, u)\|) \end{aligned} \quad (57)$$

We add zero on the right-hand side, rearrange the terms, and obtain

$$\begin{aligned} & W_\delta(m_{+,x}((x, u)|D^{dt}, X^{dt}) + w, \\ & \quad m_{+,x}((\tilde{x}, u)|D^{dt}, X^{dt}) + \tilde{w}) \\ & \leq \tilde{\eta} W_\delta(x, \tilde{x}) + \sigma_w(\|w_{1d} - \tilde{w}_{1d}\|) \\ & \quad + \sigma_h(\|h(x, u) - h(\tilde{x}, u)\|) - (\tilde{\eta} - \eta) W_\delta(x, \tilde{x}). \end{aligned}$$

Exploiting the properties of \mathcal{K} functions, the definitions of w_{1d} and \tilde{w}_{1d} from (55) - (56), and adding zero in the argument

of σ_h yields

$$\begin{aligned}
& W_\delta(m_{+,x}((x, u)|D^{dt}, X^{dt}) + w, \\
& \quad m_{+,x}((\tilde{x}, u)|D^{dt}, X^{dt}) + \tilde{w}) \\
& \leq \tilde{\eta}W_\delta(x, \tilde{x}) + \sigma_w(2\|w - \tilde{w}\|) \\
& \quad + \sigma_w(2\|e_x(x, u) - e_x(\tilde{x}, u)\|) \\
& \quad + \sigma_h(\|h(x, u) - h(\tilde{x}, u) \\
& \quad \quad + m_y((x, u)|D^{dt}, Y^{dt}) - m_y((\tilde{x}, u)|D^{dt}, Y^{dt}) \\
& \quad \quad + m_y((\tilde{x}, u)|D^{dt}, Y^{dt}) - m_y((\tilde{x}, u)|D^{dt}, Y^{dt})\|) \\
& \quad - (\tilde{\eta} - \eta)W_\delta(x, \tilde{x}) \\
& \leq \tilde{\eta}W_\delta(x, \tilde{x}) + \sigma_w(2\|(w - \tilde{w})\|) \\
& \quad + \sigma_w(2\|e_x(x, u) - e_x(\tilde{x}, u)\|) \\
& \quad + \sigma_h(2\|m_y((x, u)|D^{dt}, Y^{dt}) - m_y((\tilde{x}, u)|D^{dt}, Y^{dt})\|) \\
& \quad + \sigma_h(2\|e_y(x, u) - e_y(\tilde{x}, u)\|) - (\tilde{\eta} - \eta)W_\delta(x, \tilde{x}),
\end{aligned}$$

with e_x and e_y as defined in (33) and (34), respectively. Due to Assumption 4, we obtain

$$\begin{aligned}
& W_\delta(m_{+,x}((x, u)|D^{dt}, X^{dt}) + w, \\
& \quad m_{+,x}((\tilde{x}, u)|D^{dt}, X^{dt}) + \tilde{w}) \\
& \leq \tilde{\eta}W_\delta(x, \tilde{x}) + \sigma_w(2\|w - \tilde{w}\|) \\
& \quad + \sigma_h(2\|m_y((x, u)|D^{dt}, Y^{dt}) - m_y((\tilde{x}, u)|D^{dt}, Y^{dt})\|).
\end{aligned}$$

Since the upper and lower bounds as defined in (32a) still hold, the learned system admits a δ -IOSS Lyapunov function with $\tilde{\eta} \in [0, 1)$, $\tilde{\sigma}_w(r) = \sigma_w(2r) \in \mathcal{K}$, $\tilde{\sigma}_h(r) = \sigma_h(2r) \in \mathcal{K}$. ■